

Article

Stable Carbon Isotopes of Phytoplankton as a Tool to Monitor Anthropogenic CO₂ Submarine Leakages

Federica Relitti ^{1,2,*} , Nives Ogrinc ³ , Michele Giani ¹ , Federica Cerino ¹ ,
Mirta Smodlaka Tankovic ⁴ , Ana Baricevic ⁴ , Lidia Urbini ¹ , Bor Krajnc ³,
Paola Del Negro ¹  and Cinzia De Vittor ¹ 

¹ National Institute of Oceanography and Applied Geophysics—OGS, 34010 Sgonico (TS), Italy; mgiani@inogs.it (M.G.); fcerino@inogs.it (F.C.); lurcini@inogs.it (L.U.); pdelnegro@inogs.it (P.D.N.); cdevittor@inogs.it (C.D.V.)

² Department of Life Science, University of Trieste, 34127 Trieste, Italy

³ Department of Environmental Sciences, Jožef Stefan Institute, 1000 Ljubljana, Slovenia; nives.ogrinc@ijs.si (N.O.); bor.krajnc@ijs.si (B.K.)

⁴ Center for Marine Research, Ruder Boskovic Institute, 52210 Rovinj, Croatia; mirta@cim.irb.hr (M.S.T.); ruso@cim.irb.hr (A.B.)

* Correspondence: frelitti@inogs.it; Tel.: +39-040-2249755

Received: 29 September 2020; Accepted: 16 December 2020; Published: 19 December 2020



Abstract: This study aims to validate the stable carbon isotopic composition ($\delta^{13}\text{C}$) of phytoplankton as a tool for detecting submarine leakages of anthropogenic CO_{2(g)}, since it is characterised by $\delta^{13}\text{C}$ values significantly lower than the natural CO₂ dissolved in oceans. Three culture experiments were carried out to investigate the changes in $\delta^{13}\text{C}$ of the diatom *Thalassiosira rotula* during growth in an artificially modified medium (ASW). Three different dissolved inorganic carbon (DIC) concentrations were tested to verify if carbon availability affects phytoplankton $\delta^{13}\text{C}$. Simultaneously, at each experiment, *T. rotula* was cultured under natural DIC isotopic composition ($\delta^{13}\text{C}_{\text{DIC}}$) and carbonate system conditions. The available DIC pool for diatoms grown in ASW was characterised by $\delta^{13}\text{C}_{\text{DIC}}$ values ($-44.2 \pm 0.9\%$) significantly lower than the typical marine range. Through photosynthetic DIC uptake, microalgae $\delta^{13}\text{C}$ rapidly changed, reaching significantly low values (until -43.4%). Moreover, the different DIC concentrations did not affect the diatom $\delta^{13}\text{C}$, exhibiting the same trend in $\delta^{13}\text{C}$ values in the three ASW experiments. The experiments prove that phytoplankton isotopic composition quickly responds to changes in the $\delta^{13}\text{C}$ of the medium, making this approach a promising and low-impact tool for detecting CO_{2(g)} submarine leakages from CO_{2(g)} deposits.

Keywords: diatoms; CO₂ leakage; ¹³C; carbon fixation; Carbon Capture and Storage; Phytoplankton; CCS

1. Introduction

The 2015 Paris UNFCCC (United Nations Framework Convention on Climate Change) agreement has set the maximum global temperature increase to 2 °C to significantly reduce the risks and impacts of climate change [1]. To achieve this challenging goal, global emissions need to be reduced at about 3% year⁻¹, corresponding to 37 Gt CO_{2(g)} year⁻¹ [2]. Several strategies need to be adopted to decrease atmospheric CO_{2(g)} concentration, such as containing the rate of emissions, developing zero-carbon energy technologies, fuel-switching, improving efficiency, implementing negative emissions technologies and developing and improving carbon capture and storage (CCS) [2–4]. CCS has emerged as one of the most promising options among the mitigation technologies by storing carbon dioxide in geological reservoirs, such as depleted oil and gas fields and deep, saline formations [5], either on-shore or off-shore [4]. The International Energy Agency has assessed that, to cope with

the purpose of 2 °C warming limitation, CCS should capture about 6000 Mt CO₂ year⁻¹ by 2050, contributing 15–20% to global CO_{2(g)} emissions reduction [6]. Thus far, nineteen CCS sites are already operational [7], and, among these, six off-shore sites are currently active [8]. Although a well-engineered storage site is not expected to leak, the success and future of CCS depend on the demonstrable effectiveness of storage integrity and, therefore, on the implementation of reliable monitoring strategies for the detection of leakages and their quantification to an acceptable degree of confidence [3,9]. Geological discontinuities, abandoned exploratory boreholes and operational malfunction have been identified among the mechanisms that could potentially facilitate CO_{2(g)} leakage [10]. The dissolution of the released CO_{2(g)} in seawater leads to lower pH, and thus, it could critically affect the surrounding marine environment. Among the main adverse effects, shell formation in calcifying organisms could be inhibited, the dissolution and desorption of metals could be enhanced and, once mobilised, they can accumulate in marine organisms, interfering with physiological processes, inhibiting growth or even causing death [11–14]. Concerning primary producers, except calcareous organisms that are detrimentally affected by the dissolution of CO_{2(g)}, the contradictory effects of high dissolved CO₂ concentration have been reported [14–18]. Phytoplankton and seaweed species seem to benefit from high CO_{2(aq)} levels by enhancing the carbon and nitrogen fixation and stimulating photosynthesis [11,19,20]. However, pH decrease could affect the physiological processes of some phytoplankton species, including photosynthesis, uptake rates of trace metals and toxin production of some harmful algal species. Moreover, natural phytoplankton assemblages and community composition could be modified by high dissolved CO₂ concentrations [14]. Therefore, effective management of storage sites is required to early detect leakages and prevent risks for the surrounding environment.

Monitoring strategies have been established to detect leakages from storage sites using surface and downhole seismic methods, direct downhole measurements and seabed and water column monitoring [8,21]. Concerning the environmental monitoring, water column and sediment sampling is crucial for the chemical and geochemical characterisation of spatial and temporal dynamics of the natural baseline, thus allowing the identification of anomalies and avoiding false positive and/or negative results [21,22]. However, the temporal sampling frequency may not permit the detection of small leakages depending on plume dispersion and carbonate buffering or may not be able to cover the entire possible affected area [8]. The use of a multidisciplinary approach is encouraged; however, biological monitoring is still underutilised, though it is a low-cost effective tool [12].

Stable isotopes have been largely applied to estimate the effects of anthropogenic pressures on natural ecosystems [23]. Carbon stable isotope analysis is considered a suitable tool for tracing the fate of CO_{2(g)} in the reservoir and for detecting leakages from storage sites, provided that the isotopic composition ($\delta^{13}\text{C}$, sensu Coplen [24]) of injected CO_{2(g)} and its dissolution products is different from that of the surrounding environment [25,26]. The isotopic composition of CO_{2(g)} ($\delta^{13}\text{C}_{\text{CO}_2(\text{g})}$) stored in CCS is predominantly controlled by the $\delta^{13}\text{C}$ of the feedstock (e.g., fossil fuels, biomass and limestone) used in the CO_{2(g)}-generating process (e.g., combustion, gasification, cement and steel manufacture and fermentation) [5,27], and the $\delta^{13}\text{C}$ of most of captured CO_{2(g)} is predicted to range between –60‰ and –20‰. Despite some overlap, this range is rather distinct from the expected natural baselines; thus, $\delta^{13}\text{C}$ represents a valid geochemical tracer [27]. In particular, CO_{2(g)} derived from fossil fuels is generally characterised by $\delta^{13}\text{C}$ values similar to the isotopic composition of bulk coal (–28.46 to –23.86‰ [28]) or of methane (from –60 to –20‰ [5]) and is thus easier to be distinguished from baseline conditions.

The $\delta^{13}\text{C}$ of atmospheric CO_{2(g)} has changed significantly since the 19th century, from a value of about –6.5‰ to a present-day value below –8.0‰ as a consequence of the addition of ¹³C-depleted carbon from fossil fuel and land-use changes [29] (the so-called Suess effect [30]). $\delta^{13}\text{C}$ of the total dissolved inorganic carbon (DIC) in the ocean ranges, on average, from 0 to –2‰ [31]; however, substantial spatial-temporal variations have been detected [32,33]. Physical and biological processes affect the $\delta^{13}\text{C}$ of DIC ($\delta^{13}\text{C}_{\text{DIC}}$), resulting in relatively low values in areas of CO_{2(g)} invasion and in ¹³C-enriched DIC in areas of outgassing [33]; thus, $\delta^{13}\text{C}_{\text{DIC}}$ could range from –6.56‰ to +3.10‰ [34].

At the present marine pH, bicarbonate (HCO_3^-) is the dominant species composing DIC; therefore, its isotopic composition ($\delta^{13}\text{C}_{\text{HCO}_3^-}$) is generally very close to $\delta^{13}\text{C}_{\text{DIC}}$, whereas $\text{CO}_{2(\text{aq})}$ is ^{13}C -depleted by about $\sim 10\%$ [35], depending on the temperature isotopic fractionation and the concentrations of the carbonate species dissolved in seawater that are driven mainly by temperature, pH and salinity. Thus, the seasonal and spatial variability described for $\delta^{13}\text{C}_{\text{DIC}}$ also applies to both $\delta^{13}\text{C}_{\text{HCO}_3^-}$ and $\delta^{13}\text{C}_{\text{CO}_{2(\text{aq})}}$.

DIC uptake by primary producers represents one of the biological processes that mainly contribute to the modifications of $\delta^{13}\text{C}_{\text{DIC}}$. Indeed, during carbon uptake for photosynthesis, isotopic fractionation (ϵ , sensu Coplen [24]) occurs because of the isotopic discrimination operated by the enzyme involved in carboxylation (ribulose-1,5-bisphosphate carboxylase/oxygenase—RuBisCO). The lighter isotope ($^{12}\text{CO}_2$) is fixed at a rate 1.03 times faster than the heavier ($^{13}\text{CO}_2$), leading to ^{13}C -depleted values in phytoplankton in respect to the inorganic carbon source [36] and, consequently, enriching the residual DIC. The enzyme RuBisCO discriminates carbon by about 22‰ to 31‰, depending on the different enzyme forms that express a variable affinity for $\text{CO}_{2(\text{aq})}$ [37]. These maximum ϵ values, however, are rarely observed because several factors affect the $\text{CO}_{2(\text{aq})}$ concentration at the active site of the enzyme. These factors include the dissolved CO_2 concentration [38], phytoplankton growth rates [39,40], cell size or geometry [40], temperature and nutrient availability [41], light intensity [39,42,43], day length [44], temperature effects on enzyme kinetics [37], utilisation of HCO_3^- through CO_2 -concentrating mechanisms (CCMs) [45,46] and species variability [44,47]. Therefore, phytoplankton isotopic composition directly depends on $\delta^{13}\text{C}_{\text{DIC}}$ and its spatial and temporal variations. Phytoplankton $\delta^{13}\text{C}$ values globally range between -31.0% and -16.5% , displaying higher values in the equatorial upwelling regions and lower values at latitudes $>60^\circ$ in the northern hemisphere, and exhibit a high variability in the temperate regions due to seasonal dynamics in climatology and phytoplankton life cycle [32].

The difference between the isotopic composition of captured $\text{CO}_{2(\text{g})}$ and the natural dissolved CO_2 baseline makes $\delta^{13}\text{C}$ the most widely analysed tracer, as it allows leakage monitoring with minimal economic and environmental impacts compared to other tracers [5]. Most of the applications of the carbon stable isotope analysis are related to monitoring of the movement of injected $\text{CO}_{2(\text{g})}$ inside the reservoir [25,48–50]. The direct monitoring of the changes in $\delta^{13}\text{C}_{\text{DIC}}$ could result not suitable to detect transient leaks because of the rapid mixing in the surrounding environment of $\text{CO}_{2(\text{g})}$ leaking from a storage site. During an experimental $\text{CO}_{2(\text{g})}$ leak into the sediments of North Sea [10,51], the analysis of pore-water $\delta^{13}\text{C}_{\text{DIC}}$ allowed the identification of the leak earlier than the detection of significant changes in bicarbonate concentration [10], confirming the reliability of carbon stable isotope analysis as an inherent tracer of $\text{CO}_{2(\text{g})}$ leakage. However, it has also been highlighted that low levels of leakage may be hardly detected and quantified because of carbonate buffering and $\text{CO}_{2(\text{g})}$ transport. Phytoplankton, instead, could represent a record of the changes induced by $\text{CO}_{2(\text{g})}$ leakage, because their isotopic composition directly depends on the $\delta^{13}\text{C}$ of the available DIC pool. A considerable fraction of phytoplankton can vertically migrate along the water column to acquire multiple resources and moves towards the bottom to access the higher availability of nutrients regenerated at the sediment–water interface [52]. In a storage site, this active movement towards depth allows therefore the uptake of the $\text{CO}_{2(\text{aq})}$ that eventually leaks out. If stored $\text{CO}_{2(\text{g})}$ is characterised by $\delta^{13}\text{C}$ different than natural $\text{CO}_{2(\text{aq})}$, the phytoplankton isotopic composition is expected to significantly change from the baseline of the area that needs to be defined to take into account for the natural seasonal variability. Since stored $\text{CO}_{2(\text{g})}$ is generally characterised by $\delta^{13}\text{C}$ lower than natural $\delta^{13}\text{C}_{\text{DIC}}$, phytoplankton $\delta^{13}\text{C}$ is thus expected to change towards more negative values. An efficient CCS monitoring should therefore include, besides the geochemical analysis, the evaluation of the biological parameters that could give an integrated contribution to the detection of $\text{CO}_{2(\text{g})}$ leakages.

This study aims to explore the feasibility of using the phytoplankton stable carbon isotopic composition as a tool for detecting anthropogenic $\text{CO}_{2(\text{g})}$ leakage from the seabed. Through isotopic fractionation during photosynthetic DIC uptake, phytoplankton $\delta^{13}\text{C}$ is expected to change, thus representing an important contribution to the identification of sporadic leakages that could

not be detected by the direct analysis of the geochemical properties of the water column, provided that the isotopic composition of injected $\text{CO}_2(\text{g})$ and its dissolution products is different from that of the surrounding environment. Three pairs of culture experiments were designed in a model case approach, reproducing the isotopic composition of the carbonate system modified by an anthropogenic $\text{CO}_2(\text{g})$ submarine leakage but maintaining pH levels in the typical marine range to allow phytoplankton optimal growth. A single diatom species was grown in an artificially modified medium characterised by strongly ^{13}C -depleted dissolved CO_2 , and three different DIC concentrations were tested to verify if inorganic carbon availability would affect the phytoplankton algal metabolism. Simultaneously, at each experiment, the same diatom species was cultured under natural carbonate system and $\delta^{13}\text{C}_{\text{DIC}}$ conditions to better interpret the isotopic results considering this condition as the reference baseline.

2. Materials and Methods

2.1. Experimental Setup

Three culture experiments (EXP-1, EXP-2 and EXP-3) with the diatom *Thalassiosira rotula* were conducted within two 2L-photobioreactors (Kbiotech[®], Lugano, Switzerland) under controlled conditions of light (light:dark cycle: 14:10 h, intensity $100 \mu\text{E m}^{-2} \text{s}^{-1}$) and temperature ($20 \pm 0.02 \text{ }^\circ\text{C}$) (Figure 1 and Table 1). During each experiment, diatoms were simultaneously grown in the two bioreactors filled respectively with different media (Table 1). In one of the two bioreactors, microalgae were grown in a natural seawater medium (NAT), whereas in the second one an artificial seawater medium (ASW) was used.

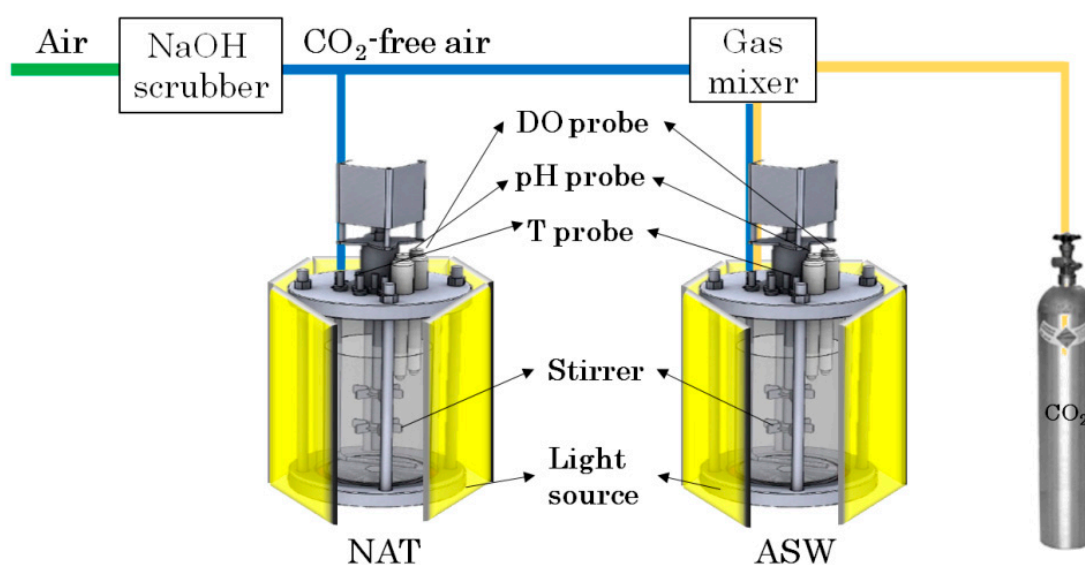


Figure 1. Schematic description of photobioreactors used for the three *T. rotula* culture experiments. NAT: natural seawater medium and ASW: artificial seawater medium. During algal growth, only CO_2 -free air was used (on:off cycle: 10:50 min) in both media. Note that $\text{CO}_2(\text{g})$ from the cylinder was only supplied during ASW medium preparation. Dissolved oxygen (DO; % sat), temperature (T; $^\circ\text{C}$) and medium pH (pH_{NBS}) were recorded by online probes. Light:dark regime: 14:10 h, continuous gentle stirring. Photobioreactor outline modified from Kbiotech[®], Lugano, Switzerland.

The ASW medium was prepared to reach a modified isotopic composition of DIC. Since $\text{CO}_2(\text{g})$ leakages from storage sites induce variations in DIC concentration, for each experiment, ASW medium was prepared differently to test whether altered DIC levels would affect the diatoms $\delta^{13}\text{C}$ in the isotopically modified environment. The different DIC concentrations tested were not coupled with pH modification; indeed, typical marine pH values (8.0–8.2) were preserved to avoid alterations in phytoplankton physiology (Table 1). DIC concentration in the ASW medium for EXP-1 (1-ASW) was

comparable to natural marine levels ($\sim 2000 \mu\text{mol L}^{-1}$), and during EXP-2 (2-ASW), about half the concentration was tested ($\sim 900 \mu\text{mol L}^{-1}$), whereas, in EXP-3 (3-ASW), more than twice the natural DIC concentration was reached ($\sim 5000 \mu\text{mol L}^{-1}$). On the other hand, the DIC concentration was maintained in the natural range ($\sim 2000 \mu\text{mol L}^{-1}$) for the three NAT experiments.

Table 1. Description of the experiments. Initial cell abundance (cells mL^{-1}) and dissolved inorganic carbon (DIC) concentration ($\mu\text{mol L}^{-1}$); initial medium pH (pH_{NBS}) and experiment duration (h) for the three experiments (EXP-1, EXP-2 and EXP-3) carried out in two bioreactors, one filled with natural seawater (NAT) and the other with artificial seawater medium (ASW).

Experiment	Medium Tested	Experiment Code	Initial Cell Abundance (Cells mL^{-1})	Initial DIC Concentration ($\mu\text{mol L}^{-1}$)	Initial pH (pH_{NBS})	Experiment Duration (h)
EXP-1	ASW	1-ASW	250	1952	8.14	96
	NAT	1-NAT	250	2222	8.32	96
EXP-2	ASW	2-ASW	1000	893	8.19	140
	NAT	2-NAT	1000	2243	8.37	140
EXP-3	ASW	3-ASW	1000	5098	8.19	120
	NAT	3-NAT	1000	2350	8.32	96

For NAT medium, a sterile-filtered (0.2- μm pore size) Adriatic Sea water was used, whereas the artificial seawater for ASW was prepared based on the artificial seawater medium ESAW (enrichment solution with artificial water) designed for coastal and open ocean phytoplankton [53], modified as follows. The solutions for the ASW medium were prepared with ultrapure Milli-Q water degassed by bubbling pure nitrogen ($\text{N}_{2(\text{g})}$) to remove the natural dissolved CO_2 . The required inorganic carbon concentrations were not achieved by the addition of sodium bicarbonate (NaHCO_3) as described in Andersen [53] recipe, because a ^{13}C -depleted DIC source needed to be reached. NaHCO_3 was replaced by a stoichiometric quantity of NaOH , and the final concentration of DIC was achieved by bubbling $\text{CO}_{2(\text{g})}$ (as a mixture of CO_2 -free air and compressed $\text{CO}_{2(\text{g})}$) into medium solution after the addition of NaOH , until the typical marine pH value was reached (8.0–8.3). Bubbling was performed with an industrial compressed $\text{CO}_{2(\text{g})}$ to achieve a modified DIC source after verifying the different isotopic composition of the gas from the current atmospheric $\delta^{13}\text{C}_{\text{CO}_{2(\text{g})}}$ ($\sim -8\text{‰}$). Since no changes in $\delta^{13}\text{C}_{\text{CO}_{2(\text{g})}}$ due to Rayleigh fractionation occurred during cylinder utilisation, the same $\text{CO}_{2(\text{g})}$ cylinder was used for the preparation of the three ASW media experiments ($\delta^{13}\text{C}$ of $\text{CO}_{2(\text{g})}$ used was $-48.2\text{‰} \pm 0.2\text{‰}$ as the average of the measurements performed during the preparation of the three different ASW media using the same gas cylinder).

Both media were supplied with nutrients and microelements, as proposed by Andersen [53] for the ESAW medium and were introduced into the photobioreactors by filtration (hydrophilic PTFE sterile filter, nominal pore size 0.2 μm , Merck KGaA, Darmstadt, Germany), with the purpose of minimising bacterial interference and to prevent gas exchange with the atmosphere.

Before the beginning of the experiments, an equal quantity of diatoms was inoculated into the two media (Table 1). A diatom species was selected, since diatoms represent the most abundant microalgae taxa worldwide due to their ability to grow in a wide range of environments and account for about 40% of marine primary production [54,55]. Moreover, carbon isotopic fractionation in diatoms is not affected by the precipitation of calcite that instead occurs in calcifying organisms [56]. The aliquot of microalgae for the inoculation was collected from clonal cultures of *Thalassiosira rotula* (species identity was confirmed by genetic analysis, Appendix A) established in September 2012 from a sample collected in the Gulf of Trieste (North Adriatic Sea) ($45^\circ 42.06' \text{ N}$, $13^\circ 42.60' \text{ E}$). The strain was maintained in 100-mL glass Erlenmeyer flasks filled with modified L1 medium obtained from sterile-filtered (0.2- μm pore size) Adriatic Sea water and supplemented with nutrients, metals and vitamins. The culture was grown at $15 \pm 2 \text{ }^\circ\text{C}$ and at a light intensity of about $53 \mu\text{E m}^{-2} \text{ sec}^{-1}$ under a controlled light:dark

regime (14:10 h). Cells were transferred within sterilised 2-L glass Erlenmeyer flasks to allow growth until the exponential phase was reached for the inoculation in the ASW and NAT media.

Periodic samplings were performed during each culture experiment through a peristaltic pump to minimise the atmospheric gas exchange. During the whole duration of the experiments, the variation of pH, temperature and dissolved oxygen was continuously monitored and recorded by online probes. Intermittent CO₂-free air flow was maintained (on:off cycle: 10:50 min), and a continuous gentle stirring prevented stratification and favoured medium mixing (Figure 1).

The duration of each experiment depended on the beginning and persistence of the stationary phase of microalgae (Table 1).

2.2. Sampling and Analysis for Phytoplankton Abundance and Media Characterisation

For phytoplankton abundance (cells mL⁻¹), an aliquot of 10 mL of culture was sampled every day and immediately fixed with prefiltered and neutralised formaldehyde (1.6% final concentration) [57]. Cell counts were performed in triplicates in a Sedgewick Rafter counting chamber at a light microscope (Leica DM2500, Leica Microsystems Srl, Wetzlar, Germany) at a magnification of 100–200×, counting a minimum of 200 cells in random fields or transects. Growth rate of the diatoms was calculated in the exponential phase of the culture [53] as

$$\mu = (\ln \text{cell}_{\text{tf}} - \ln \text{cell}_{\text{ti}}) / (t_{\text{f}} - t_{\text{i}}) \quad (1)$$

where μ (d⁻¹) is the specific growth rate, cell_{ti} represents the abundance of phytoplankton (cells mL⁻¹) at the beginning of the time interval (t_{i} ; days) in which the culture exhibited exponential growth and cell_{tf} the abundance (cells mL⁻¹) at the end of the time interval analysed (t_{f} ; days).

The pH (National Bureau of Standards, NBS, scale) was continuously recorded by online probes (EasyFerm BIO Arc 225, Hamilton Bonaduz AG, Bonaduz, Switzerland) previously calibrated on the National Bureau of Standards (NBS) scale with certified buffer solutions of pH 7 ± 0.02 and 9 ± 0.03 (at 25 °C, Merck KGaA, Darmstadt, Germany).

To measure total alkalinity (A_{T} , $\mu\text{mol kg}_{\text{SW}}^{-1}$), samples of 100-mL culture suspension were filtered over precombusted (450 °C for 4 h) Whatman (Cytiva, Global Life Sciences Solutions USA LLC, Marlborough, MA, USA) GF/F filters (nominal porosity 0.7 μm) to remove phytoplankton cells [58]. Each bottle was poisoned with saturated mercuric chloride (HgCl₂) to halt biological activity and stored at 4 °C in the dark until analysis. Total alkalinity was determined by potentiometric titration in an open cell (SOP 3b [59]), as described by Ingrosso et al. [60].

Samples for dissolved inorganic nitrogen (DIN, as the sum of nitrite—NO₂, nitrate—NO₃ and ammonium—NH₄); phosphate (PO₄) and silicate (Si(OH)₄) were filtered over precombusted (450 °C for 4 h) Whatman (Cytiva, Global Life Sciences Solutions USA LLC, Marlborough, MA, USA) GF/F filters (nominal porosity 0.7 μm) in acid-washed polyethylene vials and kept frozen (−20 °C) until laboratory analysis. Inorganic nutrient concentrations were determined calorimetrically with a QuAAtro (Seal Analytical Inc., Mequon, WI, USA) autoanalyser according to Hansen and Koroleff [61]. Detection limits reported by the analytical methods were 0.01 $\mu\text{mol L}^{-1}$, 0.02 $\mu\text{mol L}^{-1}$, 0.02 $\mu\text{mol L}^{-1}$, 0.01 $\mu\text{mol L}^{-1}$ and 0.01 $\mu\text{mol L}^{-1}$ for NO₂, NO₃, NH₄, PO₄ and Si(OH)₄, respectively. The accuracy and precision of the analytical procedures are annually checked through the quality assurance program (AQ1) QUASIMEME Laboratory Performance Studies (Wageningen, The Netherlands), and the relative coefficient of variation for five replicates was less than 5%. Internal quality control samples were used during each analysis.

Concentrations of total dissolved inorganic carbon (DIC) and the other carbonate system parameters, including dissolved CO₂ (CO_{2(aq)}) and bicarbonate (HCO₃[−]), were calculated using the CO2SYS program [62] through in situ A_{T} , medium pH (pH_{NBS} at 20 °C), temperature, salinity, phosphate and silicate data. Carbonic acid dissociation constants (i.e., pK1 and pK2) of Mehrbach et al. [63]

refitted by Dickson and Millero [64] were used for the computation, as well as the Dickson constant for the ion HSO_4^- [65] and borate dissociation constant of Uppström et al. [66].

The abundance of prokaryotes (cells mL^{-1}) was estimated by a FACSCanto II (Becton Dickinson, Franklin Lakes, NJ, USA) flow cytometer, equipped with an air-cooled laser at 488 nm and standard filter setup. Samples were treated according to Marie et al. [67], as described by Celussi et al. [68].

2.3. Sampling and Analysis of Medium and Phytoplankton Carbon Stable Isotopic Composition and Calculation of Isotopic Fractionation

Samples for the determination of the stable carbon isotope ratio of $\text{CO}_{2(\text{g})}$ of the cylinder used for ASW media preparation and the stable carbon isotope ratio of dissolved inorganic carbon (DIC) were collected in 12-mL Exetainer® (Labco Limited, Ceredigion, UK) evacuated glass tubes, preventing gas exchange with the atmosphere.

Stable carbon isotopic composition of $\text{CO}_{2(\text{g})}$ ($\delta^{13}\text{C}_{\text{CO}_{2(\text{g})}}$) was determined with an isotope ratio mass spectrometer (IRMS) Europa Scientific 20-20 (Crowe, UK) with trace gas preparation module ANCA-TG for trace gas samples.

Samples for stable isotopic composition of dissolved inorganic carbon ($\delta^{13}\text{C}_{\text{DIC}}$) were filtered over precombusted (450 °C for 4 h) Whatman GF/F filters (nominal porosity 0.7 μm) to remove phytoplankton cells, and the analysis was performed by injecting aliquots of the sample into evacuated septum tubes with phosphoric acid. Released $\text{CO}_{2(\text{g})}$ was then analysed with continuous-flow IRMS Europa 20-20 (Crowe, UK) with an ANCA-TG trace gas separation module. In order to determine the optimal extraction procedure for water samples, two standard Na_2CO_3 solutions were prepared with a known $\delta^{13}\text{C}$ value of $-10.8\text{‰} \pm 0.2\text{‰}$ and $-4.12\text{‰} \pm 0.2\text{‰}$, respectively.

The carbon isotopic composition of the phytoplankton was determined as bulk particulate organic carbon ($\delta^{13}\text{C}_{\text{POC}}$) by filtering aliquots of culture suspension (~20 mL) over precombusted (450 °C for 4 h) Whatman (Cytiva, Global Life Sciences Solutions USA LLC, Marlborough, MA, USA) GF/F filters (nominal porosity 0.7 μm , \varnothing 25 mm). To assess the potential influence of prokaryotes on the bulk $\delta^{13}\text{C}_{\text{POC}}$, other aliquots of culture suspension (~20 mL) were filtered over precombusted Whatman (Cytiva, Global Life Sciences Solutions USA LLC, Marlborough, MA, USA) GF/F filters after a prefiltration on a 10- μm nylon mesh to remove phytoplankton cells ($\delta^{13}\text{C}_{\text{POC}<10\mu\text{m}}$). The dimension of the mesh for prefiltration was chosen according to the average *Thalassiosira rotula* cell dimension of 20 μm [69]. Samples for $\delta^{13}\text{C}_{\text{POC}}$ and $\delta^{13}\text{C}_{\text{POC}<10\mu\text{m}}$ analysis were collected in duplicate, rinsed with deionised water, oven-dried at 60 °C and stored in desiccators until analysis. Before the analysis, filters for $\delta^{13}\text{C}_{\text{POC}}$ and $\delta^{13}\text{C}_{\text{POC}<10\mu\text{m}}$ were treated with 1-M HCl to remove carbonates and inserted into tin capsules for further analysis. Measurements were performed on a Europa Scientific 20-20 IRMS (Crowe, UK) with an ANCA-SL preparation module for solid and liquid samples.

All stable carbon isotope values are given conventionally in δ -notation in per mil deviation (‰) from the Vienna Peed Dee Belemnite (VPDB) standard. IRMS was calibrated against reference materials: IAEA-CH-6 and IAEA-CH-7 (International Atomic Energy Agency, Vienna, Austria) for $\delta^{13}\text{C}_{\text{POC}}$ analysis and “CO₂ ISO-TOP, High” (Messer Group GmbH, Bad Soden, Germany) with a $\delta^{13}\text{C}$ value of $-4.3 \pm 0.2\text{‰}$ for $\delta^{13}\text{C}_{\text{CO}_{2(\text{g})}}$ and $\delta^{13}\text{C}_{\text{DIC}}$. The precision based on replicate analyses was $\pm 0.2\text{‰}$ for all stable isotope analyses ($\delta^{13}\text{C}_{\text{CO}_{2(\text{g})}}$, $\delta^{13}\text{C}_{\text{DIC}}$, $\delta^{13}\text{C}_{\text{POC}}$ and $\delta^{13}\text{C}_{\text{POC}<10\mu\text{m}}$).

A mass balance relation was used to calculate the isotopic composition of dissolved $\text{CO}_{2(\text{aq})}$ ($\delta^{13}\text{C}_{\text{CO}_{2(\text{aq})}}$) and HCO_3^- ($\delta^{13}\text{C}_{\text{HCO}_3^-}$) from $\delta^{13}\text{C}_{\text{DIC}}$ by the temperature-fractionation relationships from Rau et al. [70], based on Mook et al. [35]:

$$\delta^{13}\text{C}_{\text{CO}_{2(\text{aq})}} = \delta^{13}\text{C}_{\text{DIC}} + 23.644 \frac{9701.5}{T_K}, \quad (2)$$

$$\delta^{13}\text{C}_{\text{HCO}_3^-} = \delta^{13}\text{C}_{\text{CO}_2} - 24.12 - \frac{9866}{T_K}, \quad (3)$$

where T_K is the absolute temperature in Kelvin.

Diatom isotopic fractionation associated with photosynthetic $\text{CO}_{2(\text{aq})}$ fixation was reported as the isotopic enrichment factor ($\epsilon_{\text{CO}_2\text{-POC}}$) [71] and was calculated relative to the isotopic composition of dissolved CO_2 in the bulk medium according to Farquhar et al. [72] and Freeman and Hayes [73]:

$$\epsilon_{\text{CO}_2\text{-POC}} = 1000 \frac{(\delta^{13}\text{C}_{\text{CO}_{2(\text{aq})}} - \delta^{13}\text{C}_{\text{POC}})}{(1000 + \delta^{13}\text{C}_{\text{POC}})} \quad (4)$$

Despite the presence of CO_2 -concentrating mechanisms that allow diatoms to use both HCO_3^- and $\text{CO}_{2(\text{aq})}$, the isotopic fractionation was calculated based on $\delta^{13}\text{C}_{\text{CO}_{2(\text{aq})}}$ since all inorganic carbon is converted to $\text{CO}_{2(\text{aq})}$ before being fixed and to allow for comparison with literature data.

Considering the experimental set-up, the closed-system Rayleigh-type fractionation relationships [74] were investigated to discuss the data from the natural seawater experiments by applying the following equation [71]:

$$\delta^{13}\text{C}_{\text{DIC}_t} = \delta^{13}\text{C}_{\text{DIC}_0} \times f^{(\alpha-1)}, \quad (5)$$

where $\delta^{13}\text{C}_{\text{DIC}_t}$ is the isotopic composition of the residual fraction (f) of unutilised substrate remaining ($0 \leq f \leq 1$), $\delta^{13}\text{C}_{\text{DIC}_0}$ is the isotopic composition of DIC at the beginning of the three NAT experiments (when $f = 1$ and corresponds to -2.3‰) and α is the fractionation factor and was calculated as $(\epsilon/1000) + 1$ using the theoretical value of RuBisCO isotopic fractionation (ϵ) of 20‰ [75].

To verify the possible application of the methodological approach described to CCS sites where stored $\text{CO}_{2(\text{g})}$ is characterised by different $\delta^{13}\text{C}$ values, the equation by Zhang et al. [76] for carbon isotopic fractionation during $\text{CO}_{2(\text{g})}$ dissolution in seawater was applied:

$$\epsilon_{\text{DIC-CO}_2} = 0.0144 \times T \times f\text{CO}_3^{2-} - 0.107 \times T + 10.53, \quad (6)$$

where T is the temperature in $^\circ\text{C}$ and $f\text{CO}_3^{2-}$ is the carbonate fraction of total DIC measured at the beginning of the experiments. For this calculation, the carbonate fraction measured at the beginning of the ASW experiments was used.

2.4. Statistical Analysis

The Spearman rank correlation test was used to investigate the time variation of the variables and the relationships between phytoplankton abundance, abiotic parameters and isotopic composition.

In order to verify the differences between natural and artificial seawater media and among the three experiments, the Kruskal-Wallis ANOVA test was applied to the variables. Kruskal-Wallis ANOVA and Spearman rank tests were conducted using STATISTICA 7 (StatSoft, Inc., Tulsa, OK, USA), and only significant data ($p < 0.05$ and $p < 0.01$) are presented. A multivariate analysis was performed to verify the overall difference between the two media applying a non-metric multidimensional scaling analysis (nMDS) ordination model. Phytoplankton and prokaryotes abundance data were previously square root-transformed to avoid a skewness of data that could have affected the analysis. An nMDS ordination was performed based on the triangular resemblance matrix constructed on z-normalised data using the Euclidean distance method. The analysis of similarity (one-way ANOSIM) between the ASW and NAT was also performed, and a similarity profile (SIMPROF) analysis was applied on the cluster analysis. The nMDS, ANOSIM and SIMPROF analyses were performed using PRIMER 7 (PRIMER-E Ltd., Plymouth, UK) software [77].

3. Results

3.1. Phytoplankton Growth under Different Conditions and Media Characterisation

The *Thalassiosira rotula* abundance significantly increased ($p < 0.05$) during the three experiments and nearly followed a typical exponential growth in both natural (NAT) and artificial (ASW) medium

(Figure 2). The highest abundance was measured at the end of the experiments, and the maximum value was reached in 2-ASW at 144 h ($4.17 \times 10^4 \pm 5.42 \times 10^2$ cells mL⁻¹). Despite the equal diatom inoculation in the two media at each experiment (250 cells mL⁻¹ in EXP-1, 1000 cells mL⁻¹ in EXP-2 and EXP-3; Table 1), in the ASW, the diatom growth was generally slower than in the NAT. Consequently, the exponential phase was not coincident in the two conditions, and the growth rates (μ) were not calculated in the same time interval. The stationary phase of the culture was generally achieved in the NAT (Figure 2b) within the first 48 h of the culture, and the average growth rate for the three experiments resulted in 1.1 ± 0.3 d⁻¹. On the other hand, stationary conditions in the ASW (Figure 2a) were generally reached after 72 h from the inoculation, and the average growth rate for the three experiments was 1.0 ± 0.2 d⁻¹. Despite the slight dissimilarities in growth rates, the diatom abundances between the two conditions were not significantly different. At the end of the 1-NAT experiment (96 h), the diatom abundance decreased to $1.96 \pm 0.22 \times 10^2$ cells mL⁻¹, indicating the beginning of the senescent phase. The data from this last sampling, however, were included in the discussion, since the $\delta^{13}\text{C}_{\text{POC}}$ values detected a fall in the range of the 2-NAT and 3-NAT experiments and still derived from fresh phytoplanktonic organic matter.

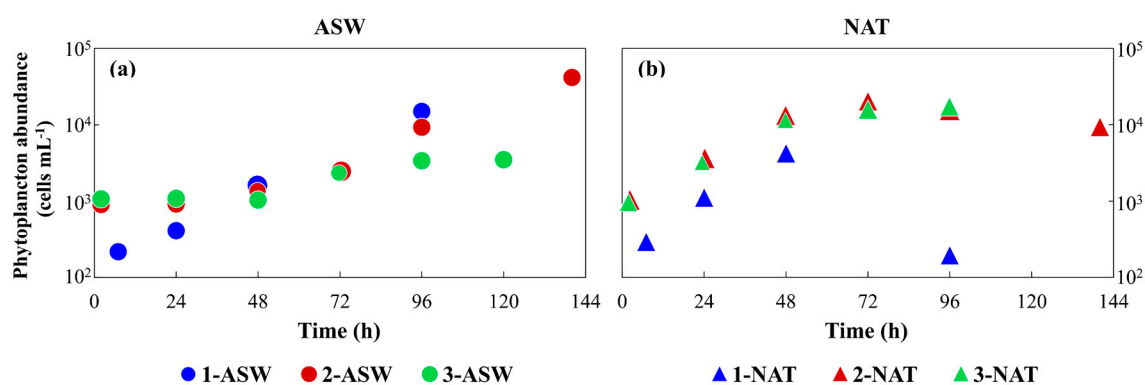


Figure 2. Time variation of *T. rotula* abundance during the three experiments of phytoplankton culture in (a) artificial seawater medium (ASW; represented by circles) and (b) natural seawater medium (NAT, represented by triangles). Blue symbols represent the first experiment (EXP-1), red the second experiment (EXP-2) and green the third experiment (EXP-3). Phytoplankton abundance is shown in a logarithmic scale.

At the beginning of the experiments, the pH levels (Figure 3a,b and Table 1) in the ASW (8.17 ± 0.03) fell within the natural marine pH range, as in the NAT (8.34 ± 0.03), suggesting that the modification in the DIC concentration induced for the ASW medium preparation did not alter pH from the natural seawater levels. A significant increase ($p < 0.05$) was observed in pH values in both media (up to 9.50; the maximum measured at 96 h in 2-NAT; Figure 3a,b). A different pattern was observed in 2-ASW (Figure 3a). In this experiment, the pH values only increased after 72 h, but the high values observed in the other two ASW experiments were not reached (2-ASW maximum pH: 8.32 at 140 h, 1-ASW maximum pH: 8.83 at 96 h and 3-ASW maximum pH: 9.12 at 96 h). Considering the whole experiments duration and excluding 2-ASW, no significant differences were detected in pH values between the NAT and ASW.

Dissolved inorganic carbon concentration in the NAT after diatom inoculation (2272 ± 68 $\mu\text{mol L}^{-1}$; Figure 3d and Table 1) fell within the typical range for the Adriatic Sea [60,78,79]. On the other hand, the DIC concentration measured in the ASW (Figure 3c and Table 1) at the beginning of the experiments confirmed the effectiveness of the modification imposed on carbonate system during the ASW medium preparation. Indeed, in 1-ASW, a typical marine DIC concentration was measured (1952 $\mu\text{mol L}^{-1}$), whereas lower (893 $\mu\text{mol L}^{-1}$) and higher (5098 $\mu\text{mol L}^{-1}$) concentrations were detected at the beginning of 2-ASW and 3-ASW, respectively. The DIC concentration significantly decreased ($p < 0.01$) in the NAT during the three experiments, reaching the minimum value at 96 h in

2-NAT ($1059 \mu\text{mol L}^{-1}$; Figure 3d). A decrease in DIC concentration was also detected in the three ASW experiments 48 h after the inoculation, reaching the lowest DIC value at 72 h in 2-ASW ($566 \mu\text{mol L}^{-1}$).

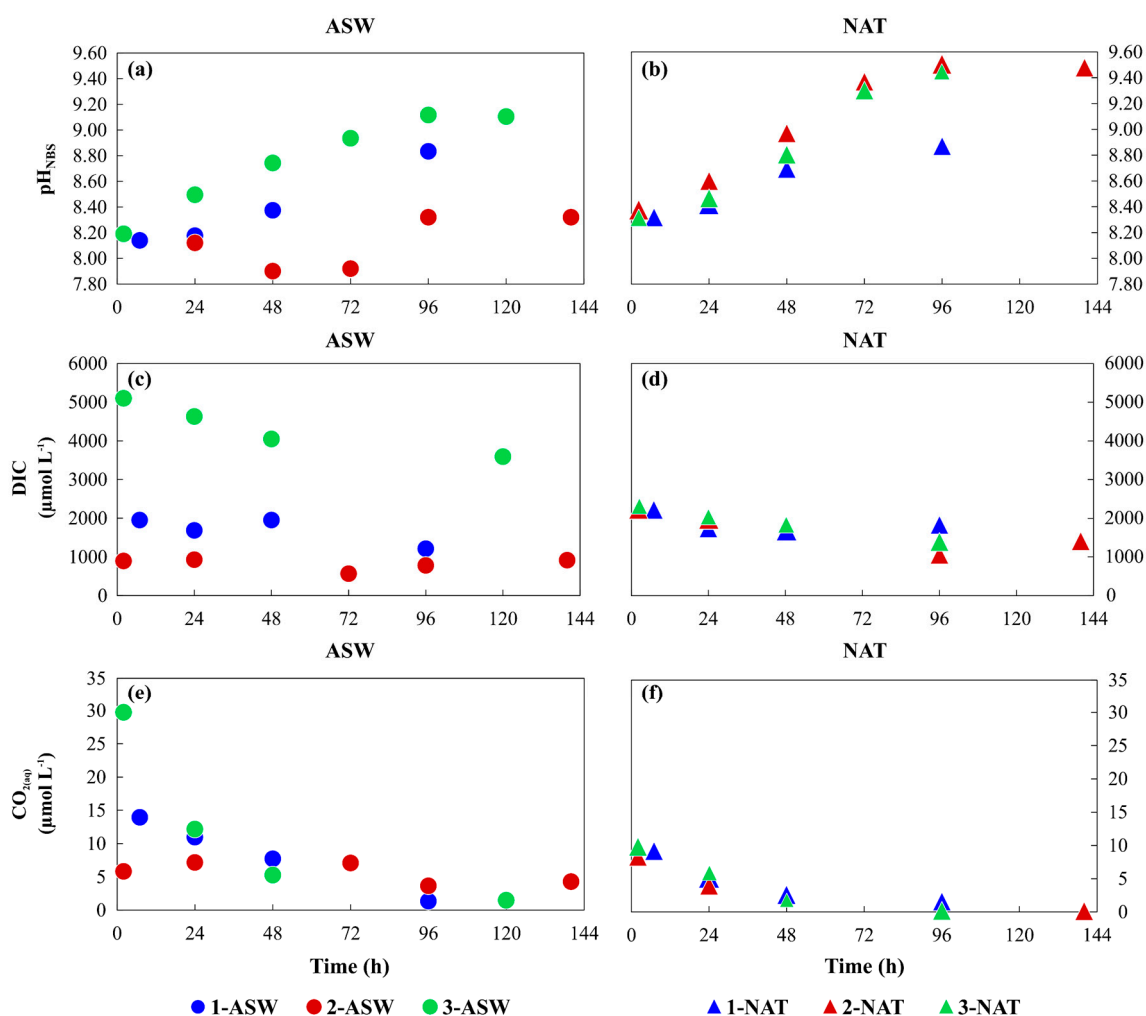


Figure 3. Time variation of the (a,b) pH_{NBS} , (c,d) dissolved inorganic carbon (DIC) and (e,f) dissolved $\text{CO}_2(\text{aq})$ during the three *T. rotula* culture experiments. Circles represent the artificial seawater medium (ASW) and triangles the natural seawater medium (NAT). Blue symbols represent the first experiment (EXP-1), red the second experiment (EXP-2) and green the third experiment (EXP-3).

The dissolved CO_2 concentration at the beginning of the three ASW experiments depended on DIC concentration (Figure 3e). Indeed, the lowest initial concentration was detected in 2-ASW ($5.81 \mu\text{mol L}^{-1}$), the highest in 3-ASW ($29.71 \mu\text{mol L}^{-1}$) and a natural marine $\text{CO}_2(\text{aq})$ concentration ($13.94 \mu\text{mol L}^{-1}$) was measured in 1-ASW. On the other hand, for the three NAT experiments, the initial $\text{CO}_2(\text{aq})$ concentration (Figure 3f) fell within the typical marine range ($9.09 \pm 0.76 \mu\text{mol L}^{-1}$). The dissolved CO_2 concentration significantly decreased ($p < 0.01$) in both the ASW and NAT during the three experiments. However, considering only 2-ASW, $\text{CO}_2(\text{aq})$ concentration remained almost constant and decreased only after 72 h. In the ASW, the minimum concentration was detected at the end of EXP-1 ($1.34 \mu\text{mol L}^{-1}$), whereas in the NAT, concentrations lower than $0.20 \mu\text{mol L}^{-1}$ were detected after 96 h in EXP-2 and EXP-3. Despite the different initial $\text{CO}_2(\text{aq})$ concentrations, considering the whole duration of the experiments, no significant differences were detected between the ASW and NAT.

3.2. Isotopic Characterisation of the Media and Phytoplankton

The initial isotopic composition of dissolved inorganic carbon ($\delta^{13}\text{C}_{\text{DIC}}$) was significantly different (Kruskal-Wallis ANOVA, $p < 0.01$) between the two conditions tested. Indeed, the initial ASW $\delta^{13}\text{C}_{\text{DIC}}$ exhibited very low values in the three experiments ($-44.2 \pm 0.9\text{‰}$; Figure 4a), whereas, in the NAT, the DIC isotopic composition ($-2.3\text{‰} \pm 1.4\text{‰}$; Figure 5b) fell within the typical range for the Adriatic Sea [79]. During diatom growth, $\delta^{13}\text{C}_{\text{DIC}}$ in the ASW (Figure 4a) significantly increased ($p < 0.01$). The minimum values were recorded at the beginning of each experiment and the maximum on the last day of the culture, reaching the highest value (-30.1‰) at 96 h in 1-ASW. No significant differences were detected among the three ASW experiments, though, in 3-ASW, $\delta^{13}\text{C}_{\text{DIC}}$ exhibited a slight increase, reaching the maximum value of -41.3‰ at the end of diatom culture (120 h). On the contrary, no significant time variations during diatom growth were detected in $\delta^{13}\text{C}_{\text{DIC}}$ in the NAT experiment (Figure 4b), with values ranging from -3.8‰ (1-NAT at 7 h) to 1.6‰ (2-NAT at 96 h).

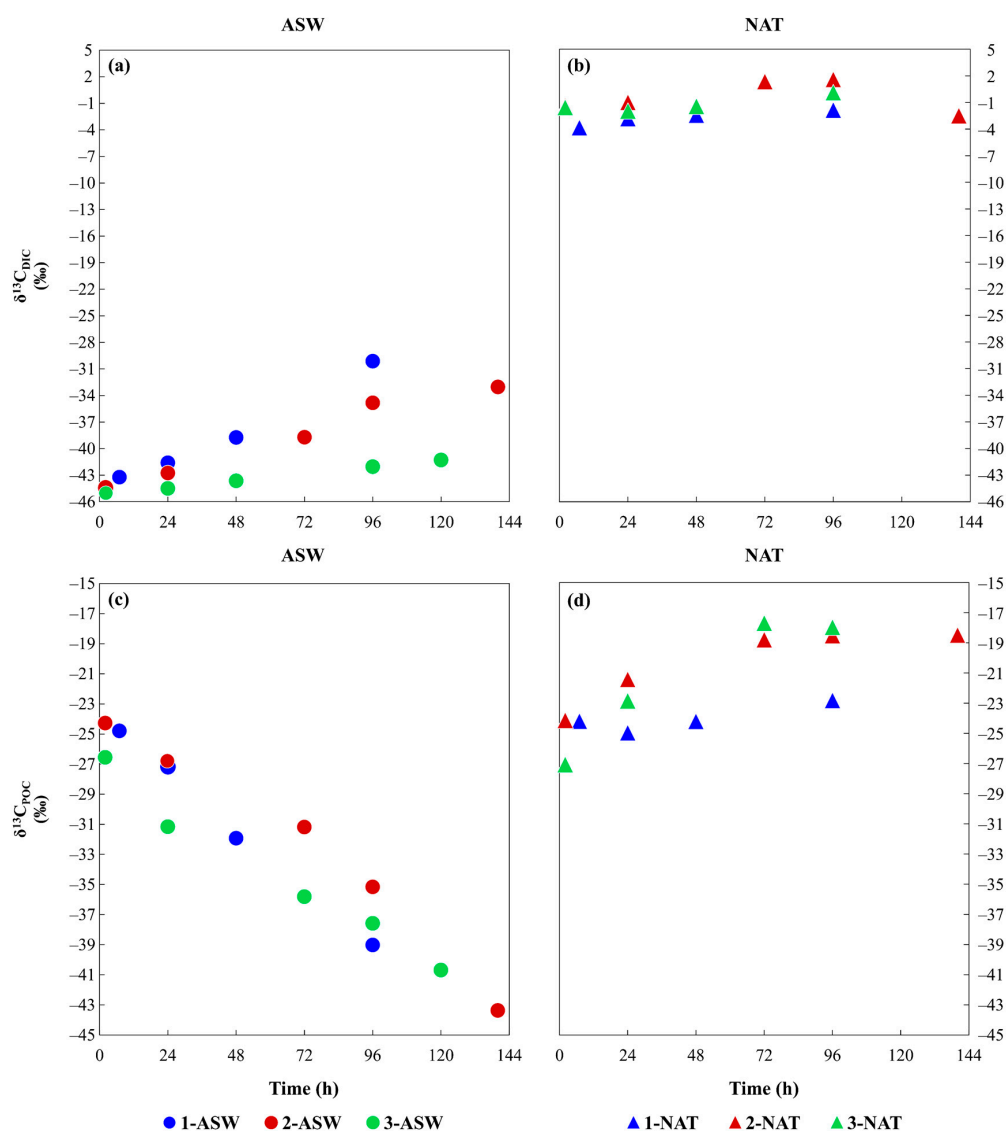


Figure 4. Time variation of the isotopic composition of (a,b) dissolved inorganic carbon ($\delta^{13}\text{C}_{\text{DIC}}$), and (c,d) phytoplankton ($\delta^{13}\text{C}_{\text{POC}}$) in the three *T. rotula* culture experiments. Circles represent the artificial seawater medium (ASW) and triangles the natural seawater medium (NAT). Blue symbols represent the first experiment (EXP-1), red the second experiment (EXP-2) and green the third experiment (EXP-3).

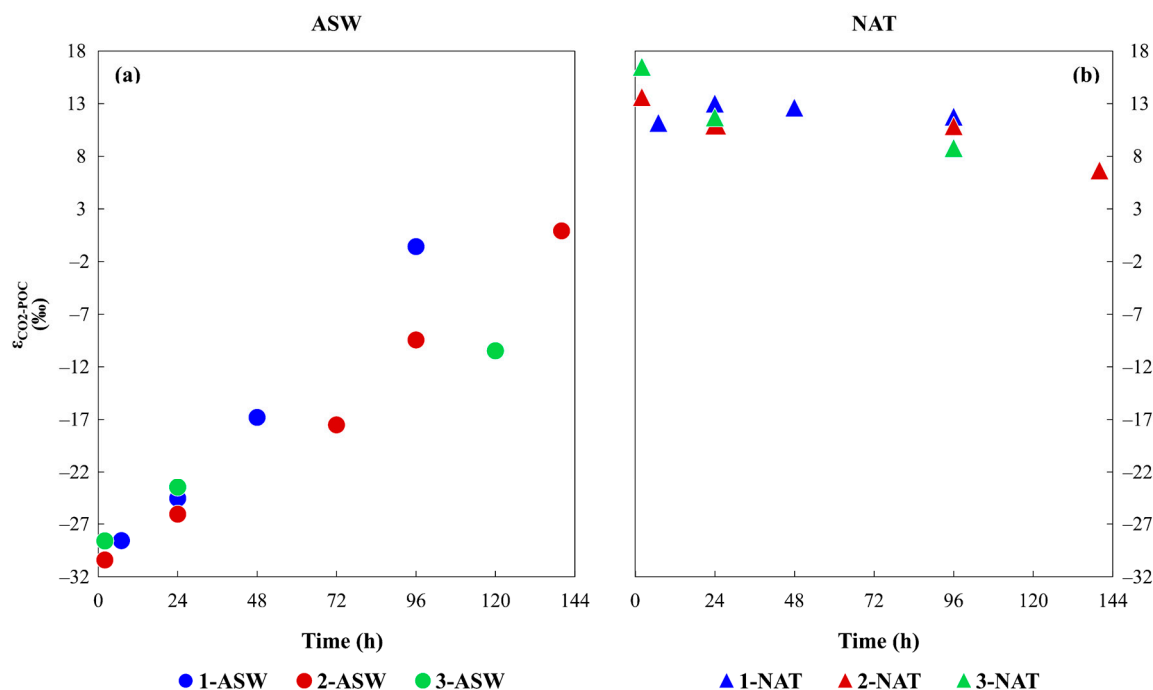


Figure 5. Time variation of the isotopic enrichment factor ($\epsilon_{\text{CO}_2\text{-POC}}$) of *T. rotula* in the three culture experiments calculated on $\delta^{13}\text{C}_{\text{CO}_2(\text{aq})}$. Circles (a) represent the artificial seawater medium (ASW) and triangles (b) the natural seawater medium (NAT). Blue symbols represent the first experiment (EXP-1), red the second experiment (EXP-2) and green the third experiment (EXP-3).

At the beginning of the culture experiments, the phytoplankton isotopic composition ($\delta^{13}\text{C}_{\text{POC}}$) did not show significant differences between the two conditions tested ($-25.2\text{‰} \pm 1.3\text{‰}$; Figure 4c,d); however, microalgae $\delta^{13}\text{C}$ exhibited an opposite trend in the ASW than NAT during the diatom growth. In the ASW (Figure 4c), the $\delta^{13}\text{C}_{\text{POC}}$ values significantly decreased ($p < 0.01$), reaching the lowest values at the end of culture experiments, until the minimum detected in 2-ASW (-43.4‰ at 140 h). On the other hand, in the NAT (Figure 4d), $\delta^{13}\text{C}_{\text{POC}}$ values slightly increased after the inoculation ($p < 0.01$), reaching the highest values at the end of the diatom culture (maximum -17.7‰ at 72 h in 3-NAT).

In the artificial seawater condition, the highest isotopic enrichment factor ($\epsilon_{\text{CO}_2\text{-POC}}$, Figure 5a) associated with $\text{CO}_2(\text{aq})$ uptake by *T. rotula* was detected at the beginning of the experiments ($-29.2\text{‰} \pm 1.0\text{‰}$). The enrichment values in the ASW significantly changed during phytoplankton growth ($p < 0.01$), reaching 0.9‰ at 140 h in 2-ASW. Slighter variations were detected in carbon isotopic enrichment in the NAT (Figure 5b), with values ranging from $13.8\text{‰} \pm 2.7\text{‰}$, calculated at the beginning of the diatom cultivation, to 6.7‰ , detected on the last day of the longest experiment (2-NAT at 140 h).

4. Discussion

4.1. Validation of the Experimental Set-Up and Diatom Growth in the Natural and Modified Media

The isotopic composition of DIC measured in ASW confirms that the experimental set-up succeeded in modifying the isotopic composition of the carbonate species dissolved in water. Indeed, $\delta^{13}\text{C}_{\text{DIC}}$ values at the beginning of ASW experiments ($-44.2\text{‰} \pm 0.9\text{‰}$) approached the isotopic composition of the strongly depleted anthropogenic $\text{CO}_2(\text{g})$ used for media preparation ($\delta^{13}\text{C}_{\text{CO}_2(\text{g})}$: $-48.2\text{‰} \pm 0.2\text{‰}$). Such low $\delta^{13}\text{C}_{\text{DIC}}$ values are hardly detected in natural systems, even in lakes where a broad range of $\delta^{13}\text{C}_{\text{DIC}}$ values is expected to be found (down to -31.1‰ [80]). On the other hand,

$\delta^{13}\text{C}_{\text{DIC}}$ in the NAT ($-2.3\text{‰} \pm 1.4\text{‰}$) fell within the typical marine range [79] and resulted significantly higher (Kruskal-Wallis ANOVA, $p < 0.01$) than values detected in the ASW.

Both the ASW and NAT were characterised by initial pH values typical for the marine environment. pH may play a significant role in limiting the rate of primary production, growth and total abundance of phytoplankton [81]. Moreover, the medium pH also affects the relative concentration of the dissolved carbonate species, thus finally conditioning the isotopic composition of $\text{CO}_{2(\text{aq})}$. It was therefore crucial to maintain comparable pH values in both the ASW and NAT in order not to affect microalgae growth and isotopic response during diatom cultivation.

Thalassiosira rotula abundances significantly increased ($p < 0.01$) in both the ASW and NAT during the three experiments (Figure 2). A general delay in microalgae growth was observed in the ASW, probably due to the acclimation time needed after the inoculation in the modified medium. However, no significant differences in terms of cell abundance were detected between the ASW and NAT.

For the ASW experiments, three different initial DIC concentrations were tested to verify the effects of lower (2-ASW; $893 \mu\text{mol L}^{-1}$) and higher (3-ASW; $5098 \mu\text{mol L}^{-1}$) DIC availability with respect to the typical marine concentration (1-ASW; $1952 \mu\text{mol L}^{-1}$). The diatom abundance was not affected by the different DIC concentrations, as no differences were detected among the three ASW experiments, and, in addition, the highest *T. rotula* abundance was detected at the end of 2-ASW, suggesting that the low DIC concentration tested during this experiment should not be limiting. These results are consistent with the experimental findings of Clark and Flynn [82] and Clark et al. [83], which showed that, at low DIC concentrations and maintaining initial pH levels in the natural range, the phytoplankton growth was not carbon limited. On the other hand, the higher availability of DIC in 3-ASW neither stimulated microalgae growth, therefore confirming that diatoms are capable of growth over a wide range of DIC availability [83]. Similar results were obtained from the mesocosm experiments performed by Maugendre et al. [84] and Esposito et al. [85], who observed no increase in phytoplankton abundance at high $\text{CO}_{2(\text{aq})}$ concentrations. Several studies indicated contrasting effects of high $\text{CO}_{2(\text{aq})}$ concentrations on the phytoplankton; indeed, the growth rates of the diatoms resulted in being stimulated, not affected or inhibited [17]. Phytoplankton growth, however, should be considered as the result of the interaction of several factors, such as pH variation, temperature, nutrients and/or light limitation, acting in synergy with the changes in the carbonate system [86]. The experiments performed by Li et al. [87] also proved that elevated $\text{CO}_{2(\text{aq})}$ has no detectable effects on the diatom *T. weissflogi* but showed limited growth and photosynthesis at lowered $\text{CO}_{2(\text{aq})}$ levels ($0.8\text{--}3.4 \mu\text{mol L}^{-1}$). However, the experiments performed by Li et al. [87] were conducted at $\text{CO}_{2(\text{aq})}$ concentrations lower than 2-ASW ($5.81 \mu\text{mol L}^{-1}$ at the beginning of the cultivation, Figure 3e) and at an initial higher pH (Li et al. [87]: $8.63\text{--}9.02$, 2-ASW: 8.19). Li et al. [87] addressed the suppression of diatom growth to the shift in carbonate system composition towards higher concentrations of HCO_3^- because of the high pH, resulting in higher energy demand for inorganic carbon uptake via concentrating mechanisms. Indeed, diatoms, as many other phytoplankton species, have developed CO_2 -concentrating mechanisms (CCMs) for actively taking up inorganic carbon and for increasing $\text{CO}_{2(\text{aq})}$ concentration around RuBisCO [88]. These mechanisms have evolved to prevent carbon limitations. The high pH of the modern sea and the slow $\text{CO}_{2(\text{aq})}$ diffusion rate in water are limiting factors for the dissolved CO_2 availability, usually making $\text{CO}_{2(\text{aq})}$ concentrations in water not sufficient to saturate RuBisCO fixation rates [88,89], representing less than 1% of total DIC [58]. CCMs increase the available inorganic carbon by active $\text{CO}_{2(\text{aq})}$ and HCO_3^- transport and by the reversible dehydration of bicarbonate to $\text{CO}_{2(\text{aq})}$ mediated by intra- and extracellular carbonic anhydrase (CA) enzymes, being $\text{CO}_{2(\text{aq})}$ the carbon species ultimately used for photosynthesis. Experimental and genetic data confirmed that both HCO_3^- and $\text{CO}_{2(\text{aq})}$ are possible substrates for diatom photosynthesis [43,88–90] and that CCMs grant full-carbon saturation of RuBisCO catalytic sites, supplementing inorganic carbon by direct HCO_3^- uptake even at high $\text{CO}_{2(\text{aq})}$ concentrations [91]. Diatoms are thus able to maintain high photosynthetic rates in response to large variations in the marine carbonate system [91]. The strain of *T. rotula* used for the experiments was cultivated from a sample collected in the Gulf of Trieste. This semi-enclosed basin is characterised

by an elevated variability in its oceanographic properties due to fluctuations in riverine inputs and climatological forcing factors that strongly affect inorganic nutrient concentrations, salinity, pH and the carbonate system [92]. Thus, the microalgae used for the experiments are adapted to a wide range of pH and variations in the carbonate system, as already reported for other coastal phytoplankton communities [17,93,94].

The inorganic carbon uptake for photosynthesis increased pH in both the ASW and NAT, and the experiments were stopped before reaching high pH levels (>9.50) that could have inhibited microalgae growth [81]. Only the 2-ASW experiment differed in pH variation, since the values detected were always lower than 8.50, and pH values increased only after the third day of diatom cultivation. This difference in pH variation could be addressed to the variation in $\text{CO}_{2(\text{aq})}$ concentration. In 2-ASW, indeed, the $\text{CO}_{2(\text{aq})}$ concentration remained almost constant for the first 72 h of the *T. rotula* cultivation. Since the diatom growth was comparable to the other experiments, it results that the carbon supply was supported by CCMs by the uptake of HCO_3^- , thus not significantly affecting the medium pH.

Diatoms were cultivated in nutrient-replete conditions (Figure S1) to avoid stress due to nutrient limitations. The DIN and PO_4 initial concentrations were comparable between the ASW and NAT, and, during diatom growth, their concentrations significantly decreased ($p < 0.05$) but were not completely consumed.

Based on the above considerations, the differences observed in phytoplankton isotopic composition between the ASW and NAT should not depend on dissimilarities in the growth conditions. Indeed, *T. rotula* should not have suffered any stress for carbon or nutrient availability during the three experiments performed. Similarly, the diatoms were not influenced by the two conditions tested, as no significant differences were detected in terms of cell abundance and growth between the NAT and ASW. Thus, the ASW and NAT $\delta^{13}\text{C}_{\text{POC}}$ values should be considered as driven mainly by the different $\delta^{13}\text{C}_{\text{DIC}}$ values.

4.2. Time Variation of Phytoplankton Isotopic Composition as a Result of Different DIC Sources and the Inorganic Carbon Uptake

The isotopic composition of phytoplankton ($\delta^{13}\text{C}_{\text{POC}}$) at the beginning of the experiments did not differ between the ASW and NAT, resulting, on average, in $-25.2\text{‰} \pm 1.3\text{‰}$. The aliquots of *T. rotula* for inoculation in the two media were sampled from the same strain of microalgae culture—thus, the similar $\delta^{13}\text{C}_{\text{POC}}$ in the two conditions at the beginning of the three experiments. The initial $\delta^{13}\text{C}_{\text{POC}}$ values in both the ASW and NAT are comparable to previous measurements performed on samples collected in the Gulf of Trieste [95,96], since the culture was prepared from a sample collected in this area and are typical for marine phytoplankton in estuarine environments.

After the inoculation in the two media, the diatoms began to uptake the DIC available, with a consequent gradual modification of the carbon isotopic composition. In the ASW, the $\delta^{13}\text{C}_{\text{POC}}$ values significantly decreased ($p < 0.01$) and reached strongly ^{13}C -depleted values at the end of the cultivation (-43.4‰ at 140 h in 2-ASW). On the other hand, in the NAT, the isotopic composition of the POC reached at the end of the experiments (-17.7‰ , the maximum measured at 72 h in 3-NAT) remained in the natural marine range and of the typical phytoplankton values measured in the open Northern Adriatic Sea (-20.6‰ [97]).

The variations of the $\delta^{13}\text{C}_{\text{POC}}$ values observed in both media depend on the isotopic fractionation due to the preferential uptake of ^{12}C for photosynthesis. If no other DIC source is available or supplied, as in the case of the experiments here described, the residual DIC pool gradually enriches in ^{13}C during the photosynthetic uptake. As also observed in mesocosm experiments [85], this typical residual source enrichment (i.e., increasing the $\delta^{13}\text{C}_{\text{DIC}}$ values) naturally occurs during intense bloom events as a consequence of the slow $\text{CO}_{2(\text{g})}$ equilibration compared to the fast biological uptake [81,86]. Both the ASW and NAT experiments reproduce a blooming condition. The diatom growth, indeed, increased the medium pH by the DIC consumption and decreased the nutrient concentration. Moreover, in the ASW, the $\delta^{13}\text{C}_{\text{DIC}}$ values increased (Figure 6a), whereas the isotopic composition of the DIC in the

NAT (Figure 6b) was not significantly modified by the diatoms carbon uptake, though the $\delta^{13}\text{C}_{\text{DIC}}$ values slightly increased (Figure 4b) during diatom cultivation. On the other hand, a clear different pattern was observed in the $\delta^{13}\text{C}_{\text{POC}}$ values between the ASW and NAT (Figure 6a,b).

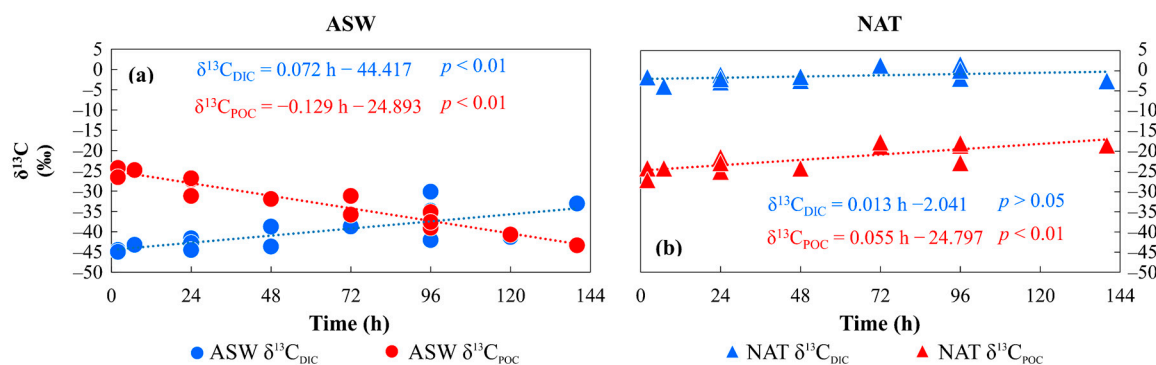


Figure 6. Comparison between the time variation of the isotopic composition of DIC ($\delta^{13}\text{C}_{\text{DIC}}$, in blue), and phytoplankton ($\delta^{13}\text{C}_{\text{POC}}$, in red) during the three *T. rotula* culture experiments in (a) artificial seawater medium (ASW) and (b) natural seawater medium (NAT). Linear regression (dashed lines) equations and correlation significance are provided in each box for both the $\delta^{13}\text{C}_{\text{DIC}}$ and $\delta^{13}\text{C}_{\text{POC}}$.

With the proceeding of diatom growth, in both the ASW and NAT, the fraction of available ^{12}C in the DIC pool gradually decreased because of the preferential uptake for photosynthesis. This process in the NAT did not change significantly $\delta^{13}\text{C}_{\text{DIC}}$ values, since the microalgae were in isotopic equilibrium with the medium. However, considering the fast growth of microalgae, the gradual reduction of the ^{12}C in the available DIC resulted in an evident ^{13}C -enrichment of the phytoplankton with increasing $\delta^{13}\text{C}_{\text{POC}}$ values during diatom growth (Figure 6a). In the ASW, despite the significant increase ($p < 0.01$) in $\delta^{13}\text{C}_{\text{DIC}}$ values, as the result of the preferential uptake of the ^{12}C by the diatoms, the $\delta^{13}\text{C}_{\text{POC}}$ values showed an opposite behaviour than in the NAT (Figure 6a). This misleading isotopic anomaly depended on the source of DIC provided in the ASW and on the experimental set-up. The experiments aimed to verify how the isotopic composition of the diatoms changed during the growth in a modified medium; therefore no acclimation time followed the inoculation. The *Thalassiosira rotula* strain was grown under natural marine $\delta^{13}\text{C}_{\text{DIC}}$ until inoculation, and once transferred in the ASW medium, microalgae started to take up the modified DIC available. As discussed in the previous section (Section 4.1), the ASW was characterised by low $\delta^{13}\text{C}_{\text{DIC}}$ values; therefore, the lightest isotope (^{12}C) was much more abundant than in the NAT. The diatoms had therefore a higher availability of ^{12}C for photosynthesis, and this resulted in the significant ($p < 0.01$) and quick decrease in $\delta^{13}\text{C}_{\text{POC}}$ values (Figure 6a) and the following increase in $\delta^{13}\text{C}_{\text{DIC}}$. Notwithstanding that the variation of $\delta^{13}\text{C}_{\text{DIC}}$ during diatom growth was similar in all ASW experiments, in 3-ASW, a slighter increase was observed. The culture medium for 3-ASW was prepared to obtain high DIC concentration (Figure 3c); consequently, ^{12}C was even more abundant than in 2-ASW and 1-ASW. Since the diatom growth and $\delta^{13}\text{C}_{\text{POC}}$ followed the same trend as 1-ASW and 2-ASW, the residual DIC in 3-ASW maintained a relatively higher amount of ^{12}C than the other ASW experiment during the *T. rotula* culture; therefore, a slighter variation was observed in the $\delta^{13}\text{C}_{\text{DIC}}$.

Esposito et al. [85] found a similar decrease in $\delta^{13}\text{C}_{\text{POC}}$ values during mesocosm experiments after the addition of seawater bubbled with ^{13}C -depleted $\text{CO}_{2(\text{g})}$. The POC isotopic composition reflected the trend of $\delta^{13}\text{C}_{\text{DIC}}$, and the minimum $\delta^{13}\text{C}_{\text{POC}}$ was reached at the end of the experiments, although higher values than those measured in our experiments were reached. To our knowledge, extremely low $\delta^{13}\text{C}_{\text{POC}}$ values, similar to those detected at the end of our experiments, were only measured by Poulain et al. [98] ($-58\text{‰} \pm 4\text{‰}$) in a mixed-species phytoplankton culture (used as a zooplankton food source) grown in a medium where ^{13}C -depleted industrial $\text{CO}_{2(\text{g})}$ was bubbled, even though additional medium information (e.g., pH, DIC concentration and $\text{CO}_{2(\text{g})}$ bubbling duration) was not provided to allow additional consideration.

The isotopic composition of *T. rotula* in the ASW resulted significantly different (Kruskal-Wallis ANOVA, $p < 0.01$) from that of diatoms grown in the NAT. The inverse correlation ($p < 0.01$) of $\delta^{13}\text{C}_{\text{POC}}$ with both $\delta^{13}\text{C}_{\text{DIC}}$ and diatom abundance in the ASW supports the hypothesis that the isotopic composition of *T. rotula* depends mostly on the isotopic composition of the available DIC source. The different DIC concentrations in the ASW experiments seem not to affect the final phytoplankton $\delta^{13}\text{C}$, as no significant differences were detected in $\delta^{13}\text{C}_{\text{POC}}$ among the three ASW experiments, confirming that the DIC concentration is not becoming a limiting factor and does not affect the $\delta^{13}\text{C}_{\text{POC}}$ [99,100].

The presence of prokaryotes was monitored to consider its potential effect on the bulk POC isotopic composition, since the prokaryotes abundance increased ($p < 0.05$, Figure S2) in both media throughout the duration of the experiments. The isotopic composition of the fraction of POC smaller than $10\ \mu\text{m}$ ($\delta^{13}\text{C}_{\text{POC}<10\mu\text{m}}$), assumed to depend mostly on the prokaryotes biomass, followed the same trend as $\delta^{13}\text{C}_{\text{POC}}$ ($p < 0.01$) in both the ASW and NAT. Previous studies [101,102] revealed that the heterotrophic prokaryotes isotopic composition is generally close to or similar to that of the organic substrate provided. This is consistent with the results here discussed, because, during algal growth in bioreactors, the only substrate for prokaryotes was the phytoplankton-derived organic matter [103]. Slighter variations, however, were observed in $\delta^{13}\text{C}_{\text{POC}<10\mu\text{m}}$ compared to $\delta^{13}\text{C}_{\text{POC}}$ during phytoplankton growth as the result of a delay in the incorporation of the freshly produced phytoplankton material, as already discussed by De Kluijver et al. [104] in labelling experiments. Considering the strong positive correlation between $\delta^{13}\text{C}_{\text{POC}<10\mu\text{m}}$ and $\delta^{13}\text{C}_{\text{POC}}$ in both the ASW and NAT, it could be therefore assumed that the increase in prokaryotes biomass might have been not sufficient to modify the bulk POC isotopic composition.

A multivariate analysis (nMDS; Figure 7) was performed to investigate the global difference between the two conditions tested. The isotopic composition of POC, DIC and $\delta^{13}\text{C}_{\text{POC}<10\mu\text{m}}$, phytoplankton and prokaryotes abundances, pH and inorganic nutrients were the parameters included in the analysis. Considering the time variation of $\delta^{13}\text{C}_{\text{POC}}$ and the comparability of the diatom abundance in the three ASW experiments, it was concluded that the different DIC concentrations tested did not affect the phytoplankton carbon uptake; therefore, neither DIC nor $\text{CO}_{2(\text{aq})}$ concentrations were included in the nMDS analysis to avoid the strong effect of the different concentrations tested in the analysis. Two groups can be clearly distinguished (Figure 7), and the separation corresponds to the two different media in which the diatoms were grown (ASW and NAT). The strongest separation of the groups was evident at the final sampling times, when the highest difference in $\delta^{13}\text{C}_{\text{POC}}$ values was detected between the ASW and NAT. The analysis of similarity (one-way ANOSIM) supported the significant global differences between ASW and NAT ($p < 0.05$), even if with a certain degree of overlapping of the data ($R = 0.358$) probably related to the common starting condition of the microalgae culture. Indeed, the SIMPROF analysis highlighted as a unique group the data collected within the first day of cultivation, whereas the separation of the NAT and ASW became gradually wider following the phytoplankton growth in the two culture media.

The multivariate analysis confirmed that carbon stable isotopes could be considered as valid tracers of the origin of dissolved inorganic carbon. Indeed, both the $\delta^{13}\text{C}_{\text{DIC}}$ and $\delta^{13}\text{C}_{\text{POC}}$ values significantly depend on the different origin of dissolved CO_2 , and phytoplankton $\delta^{13}\text{C}$ quickly responded to the change of growth medium. The time variation of phytoplankton $\delta^{13}\text{C}$ in the ASW experiments resulted in a decrease of $\sim 3.1\text{‰}$ (calculated from the regression line, Figure 6a) in only one day of cultivation, corresponding to an average ^{13}C -depletion of $\sim 18\text{‰}$ in less than one week. Conversely, the derived increase in $\delta^{13}\text{C}_{\text{DIC}}$ corresponded to $\sim 1.7\text{‰ d}^{-1}$ (Figure 6a), which is comparable to the increasing trend identified for $\delta^{13}\text{C}_{\text{POC}}$ in the NAT ($\sim 1.4\text{‰ d}^{-1}$, Figure 6b). The modification of the phytoplankton isotopic composition in the diatoms grown in the ASW is, therefore, faster and broader than the variation of medium $\delta^{13}\text{C}_{\text{DIC}}$. These results are consistent with the mesocosm experiments performed by Esposito et al. [85] that highlighted a significant drop of $\delta^{13}\text{C}_{\text{POC}}$ values in the ^{13}C -depleted mesocosm about five days after the bloom phase. The $\delta^{13}\text{C}_{\text{POC}}$ decrease observed by Esposito et al. [85]

is comparable to the POC ^{13}C -depletion in the ASW after ~ 1.5 days, confirming that our experimental approach is able to fast detect changes in the phytoplankton isotopic composition.

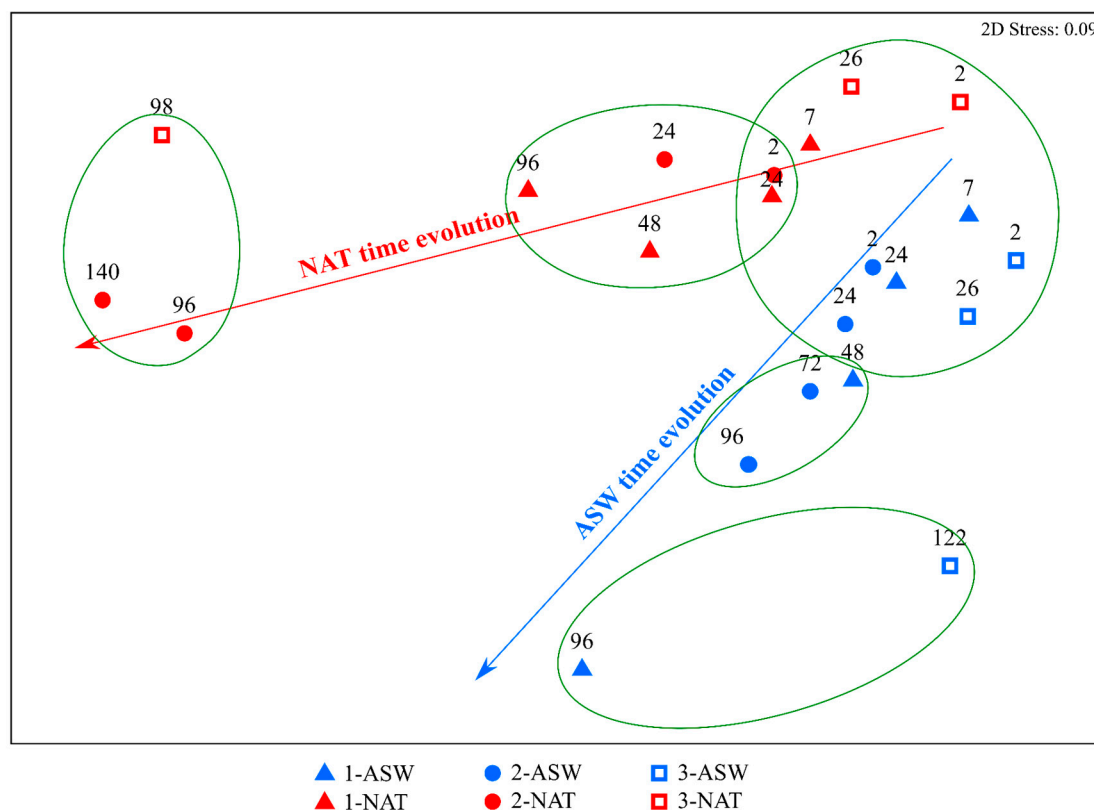


Figure 7. Nonmetric multidimensional scaling analysis (nMDS) of the *T. rotula* culture experiments. The first experiment (EXP-1) is represented by triangles, the second (EXP-2) by circles and the third (EXP-3) by squares. Blue symbols represent the artificial seawater medium (ASW), and red symbolises the natural seawater medium (NAT). Numbers above the symbols represent the sampling time (h). The green lines represent the groups identified by the similarity profile (SIMPROF) analysis.

This result should be considered when dealing with $\text{CO}_2(\text{g})$ leakages from storage sites. In a real CCS site, the chemical composition of the water column quickly changes after a leakage, and $\delta^{13}\text{C}_{\text{DIC}}$ is modified depending on the $\text{CO}_2(\text{g})$ concentration released and on the environmental conditions. However, the $\delta^{13}\text{C}_{\text{DIC}}$ values return to background levels due to mixing currents that rapidly disperse $\text{CO}_2(\text{g})$ both horizontally and vertically [11]. Therefore, a $\text{CO}_2(\text{g})$ leakage could be detected by $\delta^{13}\text{C}_{\text{DIC}}$ analysis only if the sampling is close enough in time. On the other hand, considering the rapid variation of diatom $\delta^{13}\text{C}$, the assessment of $\text{CO}_2(\text{g})$ leakages through the analysis of the isotopic composition of phytoplankton gives the opportunity to gather time-integrated information, and thus, even low and sporadic emissions, that otherwise would be hardly detectable from the seawater analysis, could be identified.

4.3. Phytoplankton Isotopic Fractionation

The isotopic composition of phytoplankton depends on the fractionation occurring during inorganic carbon uptake [73] and was described as isotopic enrichment factor ($\epsilon_{\text{CO}_2\text{-POC}}$) [71]. Isotopic fractionation is mainly the result of the activity of the enzyme RuBisCO during photosynthetic $\text{CO}_2(\text{aq})$ fixation, which discriminates carbon by about 22‰ to 31‰, depending on the $\text{CO}_2(\text{aq})$ affinity of the different RuBisCO forms [37], thus resulting in ^{13}C -depleted values in the phytoplankton. However, these maximum $\epsilon_{\text{CO}_2\text{-POC}}$ values are rarely observed, because several physiological and environmental factors affect $\text{CO}_2(\text{aq})$ concentration at the active site of the enzyme [37–47].

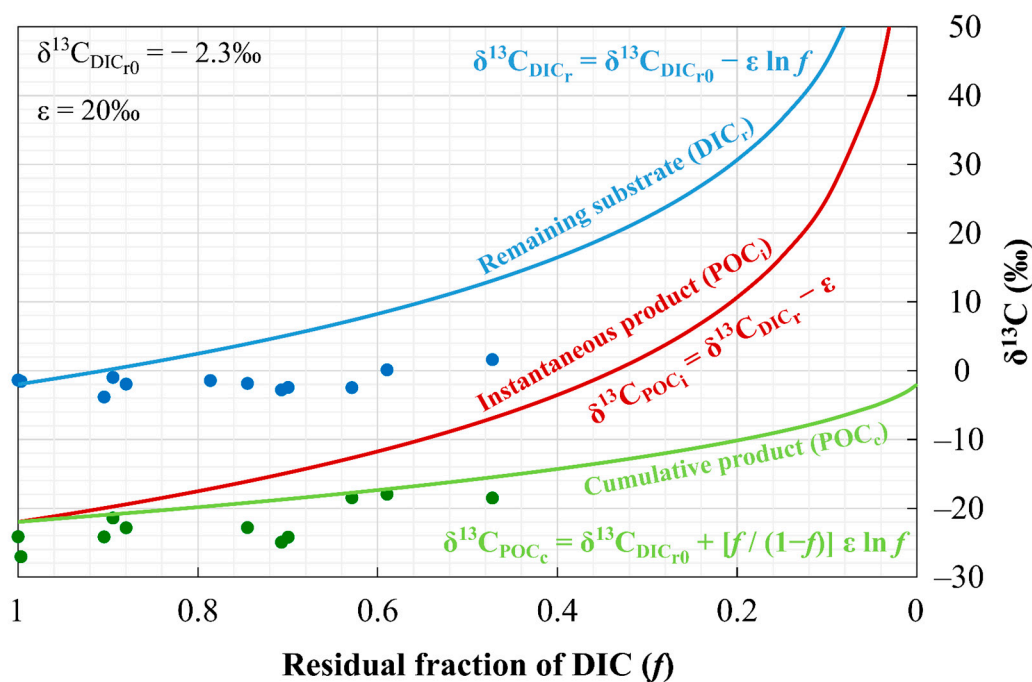
For the experiments here discussed, a single diatom species—*Thalassiosira rotula*—was grown in two different media (ASW and NAT) under equal conditions of light availability, temperature and nutrient concentration. Since *T. rotula* growth was similar in the ASW and NAT (Section 4.1), the significant differences (Kruskal-Wallis ANOVA, $p < 0.01$) of the $\epsilon_{\text{CO}_2\text{-POC}}$ values detected between the two conditions tested should be addressed to the different isotopic composition of the phytoplankton and DIC and, eventually, to the availability of $\text{CO}_2(\text{aq})$, even if the DIC concentration seemed not to affect either the diatom growth or its isotopic composition (Sections 4.1 and 4.2).

Extremely negative $\epsilon_{\text{CO}_2\text{-POC}}$ values were calculated in the artificially modified medium ($-29.2\text{‰} \pm 1.0\text{‰}$) at the beginning of the experiments, and an increasing trend ($p < 0.01$) was observed during diatom growth. These low values depend on the experimental setup, since aliquots of *T. rotula* were inoculated into a strongly ^{13}C -depleted medium without an acclimation period; thus, after inoculation, the diatom $\delta^{13}\text{C}$ values were higher than $\delta^{13}\text{C}_{\text{DIC}}$. The largest availability of ^{12}C and the quick utilisation of DIC in the ASW experiments resulted in negative $\epsilon_{\text{CO}_2\text{-POC}}$ values that progressively increased during algal growth as a consequence of the gradual reduction in the difference between the source (DIC) and product (POC) isotopic compositions. A switch to positive $\epsilon_{\text{CO}_2\text{-POC}}$ values was observed after 96 h of cultivation due to the modifications induced in $\delta^{13}\text{C}_{\text{DIC}}$ and $\delta^{13}\text{C}_{\text{POC}}$ because of the DIC uptake (Figure 5a).

The isotopic enrichment in the natural medium, on the contrary, was characterised by decreasing values ($p < 0.05$), following the gradual ^{13}C -enrichment of the DIC pool because of the uptake of ^{12}C for photosynthesis [105]. The $\epsilon_{\text{CO}_2\text{-POC}}$ values in the NAT (13.8~6.7‰) were lower than the in vitro RuBisCO ϵ -values calculated for the marine diatom *Skeletonema costatum* (18.5‰ [106]) but fell in the range of the measurements performed in a mesocosm experiment (9.6~16.5‰ [85]) where diatom was the predominant phytoplankton taxon.

As previously discussed, DIC concentration does not affect the phytoplankton isotopic composition; however, the observed decrease in $\epsilon_{\text{CO}_2\text{-POC}}$ values in the NAT are consistent with previous studies demonstrating that phytoplankton ^{13}C -discrimination is lower the less DIC is available [105,107]. On the other hand, a higher carbon supply is expected to induce more pronounced isotopic fractionation (i.e., an increase in $\epsilon_{\text{CO}_2\text{-POC}}$ values) [85,107,108]. The results from the 3-ASW experiment, in which a higher DIC concentration was tested, are in contrast with this assumption. Indeed, no differences were detected in the $\epsilon_{\text{CO}_2\text{-POC}}$ values in the ASW experiments due to the different DIC availability, showing that the only change in the DIC concentration did not have a large effect on the $\delta^{13}\text{C}_{\text{POC}}$, as also recently reported by Tuerena et al. [99]. In both the ASW and NAT, the $\epsilon_{\text{CO}_2\text{-POC}}$ values were strongly correlated with $\delta^{13}\text{C}_{\text{POC}}$ ($p < 0.01$) and diatom abundance ($p < 0.05$); thus, the microalgae growth and the carbon isotopic fractionation occurring during photosynthetic DIC uptake should be considered the main drivers for the variations observed in the phytoplankton $\delta^{13}\text{C}$.

The theoretical relationship between the isotopic composition of the phytoplankton and DIC in the natural seawater experiments was investigated by applying the closed-system Rayleigh-type fractionation model [109]. The isotopic fractionation associated with the DIC uptake was assumed to correspond to the theoretical value of RuBisCO isotopic fractionation (ϵ) of 20‰ [75]. The resulting relationships between the $\delta^{13}\text{C}$ of the cumulative POC (green curve), source carbon (DIC, blue curve) and incremental POC (red curve) are shown in Figure 8, together with the experimental $\delta^{13}\text{C}_{\text{POC}}$ (green circles) and $\delta^{13}\text{C}_{\text{DIC}}$ (blue circles) data from the three NAT experiments. According to the literature data, the enzymatic isotopic fractionation can vary between 22‰ and 31‰ [37]; however, by applying any other isotopic fractionation value included in this range the shape of the lines does not significantly change.



- NAT experimental $\delta^{13}\text{C}_{\text{DIC}}$ values
- NAT experimental $\delta^{13}\text{C}_{\text{POC}}$ values

Figure 8. Closed-system Rayleigh-type fractionation relationship calculated for the three *T. rotula* culture experiments in the natural seawater medium (NAT). The isotopic composition of the residual fraction (f ; $0 \leq f \leq 1$) of unutilised substrate remaining (DIC_r) is represented by the blue line ($\delta^{13}\text{C}_{\text{DIC}_r}$), and the isotopic composition of the cumulative (POC_c) and instantaneous (POC_i) products are shown by the green ($\delta^{13}\text{C}_{\text{POC}_c}$) and red ($\delta^{13}\text{C}_{\text{POC}_i}$) lines, respectively. The experimental data of the $\delta^{13}\text{C}_{\text{POC}}$ and $\delta^{13}\text{C}_{\text{DIC}}$ from the three NAT experiments are also plotted as green circles and blue circles, respectively. The mathematical formulae for reactants and products are shown [110].

The experimental results of the $\delta^{13}\text{C}_{\text{POC}}$ (green circles) plot in-line with the cumulative product (green line), while the $\delta^{13}\text{C}_{\text{DIC}}$ data (blue circles) plot out of the source carbon curve (blue line); thus, the processes occurring in the system cannot be described only by the closed-system Rayleigh-type fractionation model. Indeed, the literature data indicate that the photosynthetic ^{13}C fractionation can be described as a passive-diffusion phytoplankton photosynthesis, where the isotopic fractionation is associated with diffusive transport of $\text{CO}_{2(\text{aq})}$ and enzymatic, intracellular carbon fixation [45,70]. Furthermore, the phytoplankton $\delta^{13}\text{C}$ values are not solely controlled by the $\text{DIC}/\text{CO}_{2(\text{aq})}$ concentrations, but several factors both physiological (e.g., phytoplankton growth rates and cell dimension) and environmental (e.g., temperature, nutrient concentration and light intensity) [39,42–44,70] affect the isotopic fractionation. Indeed, during the experiments, the $\varepsilon_{\text{CO}_2\text{-POC}}$ values were not constant either in the ASW or in the NAT. Moreover, the presence of CCMs in diatoms allows the uptake of both $\text{CO}_{2(\text{aq})}$ and HCO_3^- [88,89]. Intra- and extracellular carbonic anhydrase (CA) enzymes have been recognised to operate in the reversible dehydration of bicarbonate to $\text{CO}_{2(\text{aq})}$, since it is the species ultimately used for photosynthesis. Bicarbonate is relatively ^{13}C -enriched in respect to $\text{CO}_{2(\text{aq})}$ by about $\sim 10\%$ [35], but a comparable kinetic fractionation occurs during the dehydration of bicarbonate by CA, making CA-mediated HCO_3^- uptake indistinguishable from direct $\text{CO}_{2(\text{aq})}$ uptake [111] from an isotopic point of view. However, if no HCO_3^- leaks out of the cell and all the bicarbonate taken up is converted into $\text{CO}_{2(\text{aq})}$, no fractionation occurs during the process of intracellular dehydration, making the substrate for photosynthesis 9–10‰ enriched than $\text{CO}_{2(\text{aq})}$, thus affecting the resulting phytoplankton isotopic $\varepsilon_{\text{CO}_2\text{-POC}}$ values [112]. In this process, pH was identified as an important controlling factor, since it regulates the level of CA activity, the induction of CCMs and affects carbon leakage from the cell

in relation to the $\text{CO}_{2(\text{aq})}$ and HCO_3^- uptake and conversion [112]. The increase in pH detected in both conditions during diatom growth has clearly moved the carbonate system equilibrium towards higher concentrations of bicarbonate; thus, both in the ASW and NAT, HCO_3^- should have played an important role as a photosynthetic substrate. No differences were encountered in the pH trend between the ASW and NAT; hence, the bicarbonate contribution should have been comparable and, thus, should not cover a significant role in the interpretation of the differences detected in $\delta^{13}\text{C}_{\text{POC}}$. Moreover, as discussed in Section 4.1, in 2-ASW, the pH variation was slighter, and a lower DIC concentration was tested, implying that the contribution of HCO_3^- was reduced compared to the other experiments performed. However, the $\delta^{13}\text{C}_{\text{POC}}$, $\delta^{13}\text{C}_{\text{DIC}}$ and, thus, $\epsilon_{\text{CO}_2\text{-POC}}$ values followed the same trend as 1-ASW and 3-ASW, confirming that the different origin of $\text{CO}_{2(\text{aq})}$ (i.e., the different isotopic composition) was the main factor affecting the phytoplankton isotopic composition and that the variation in DIC concentration and of the contribution of the different carbonate species did not significantly affect the diatom isotopic composition.

4.4. Application of the Method to CCS Sites: Limitations and Future Perspectives

The available DIC pool for diatoms grown in the artificially modified medium was characterised by $\delta^{13}\text{C}_{\text{DIC}}$ values significantly different from the typical marine range. Through photosynthetic isotopic fractionation, the microalgae isotopic composition rapidly changed, reaching significantly ^{13}C -depleted values (decrease of $\sim 3.1\%$) in just one day. Moreover, the modification of diatom $\delta^{13}\text{C}$ resulted not affected by the different concentrations of dissolved inorganic carbon, exhibiting the same trend in $\delta^{13}\text{C}_{\text{POC}}$ values for all the DIC concentrations tested.

The results of the experiments described are encouraging for the future application of this method as a monitoring approach at CCS sites. However, the condition tested represents an extreme case, and further experiments should be performed. The $\delta^{13}\text{C}_{\text{CO}_2(\text{g})}$ used for the ASW experiments simulates the leakage of stored $\text{CO}_{2(\text{g})}$ derived from fossil fuels combustion. However, the different feedstocks and $\text{CO}_{2(\text{g})}$ -generating processes are expected to expand the range of stored $\delta^{13}\text{C}_{\text{CO}_2(\text{g})}$ values [5,27]. The first requirement for the application of the approach described is that $\delta^{13}\text{C}_{\text{DIC}}$ values after $\text{CO}_{2(\text{g})}$ leakage are significantly different from the natural baseline. To test whether different $\delta^{13}\text{C}_{\text{CO}_2(\text{g})}$ leaking would result in detectable differences, the equation for carbon isotope fractionation during $\text{CO}_{2(\text{g})}$ dissolution in seawater by Zhang et al. [76] (Equation (6), Section 2.3) was applied using different $\delta^{13}\text{C}_{\text{CO}_2(\text{g})}$ values and assuming the atmospheric $\delta^{13}\text{C}_{\text{CO}_2(\text{g})}$ corresponding to -8.0% . The different $\delta^{13}\text{C}$ of leaking $\text{CO}_{2(\text{g})}$ tested were -15.0% , -20.0% , -25.0% and -35.0% . The equation was also applied to the $\delta^{13}\text{C}$ value of $\text{CO}_{2(\text{g})}$ used for the three ASW media preparations (-48.2%) (Figure 9).

To assess more confidently whether this approach would be useful on specific CCS sites, the natural baseline must be defined in detail to verify if the variations in $\delta^{13}\text{C}$ of the DIC and phytoplankton would overlap with the natural seasonal variations. The detection of leakages would be more difficult if $\delta^{13}\text{C}_{\text{DIC}}$ values resulting from leaking $\text{CO}_{2(\text{g})}$ dissolution were similar to the natural baseline. Among the different $\delta^{13}\text{C}_{\text{CO}_2(\text{g})}$ values tested, leaking $\text{CO}_{2(\text{g})}$ characterised by a $\delta^{13}\text{C}$ of -15% represents the worst scenario to be distinctly detected by isotopic analysis. In that case, if the natural $\delta^{13}\text{C}_{\text{DIC}}$ in the CCS area can reach the lowest value of -4% , the leakage would be detectable if its concentration would finally correspond to at least 70% of the total DIC (Figure 9). On the other hand, if $\delta^{13}\text{C}_{\text{DIC}}$ naturally never reaches values lower than -1% , the leakage might be detectable if it corresponds to 40% of the total DIC (Figure 9). The resulting differences in phytoplankton isotopic composition are much more complicated to be modelled, since several factors affect fractionation during photosynthesis [37–47,70]. Obviously, if the leaking $\text{CO}_{2(\text{g})}$ dissolution results in significant differences in $\delta^{13}\text{C}_{\text{DIC}}$ values in respect to the natural baseline, also significant differences in $\delta^{13}\text{C}_{\text{POC}}$ are expected accordingly. Therefore, for the correct implementation of this method, it is important to know the natural variations of $\delta^{13}\text{C}_{\text{DIC}}$ and $\delta^{13}\text{C}_{\text{POC}}$ at the storage site and the isotopic composition of stored $\text{CO}_{2(\text{g})}$ at the CCS.

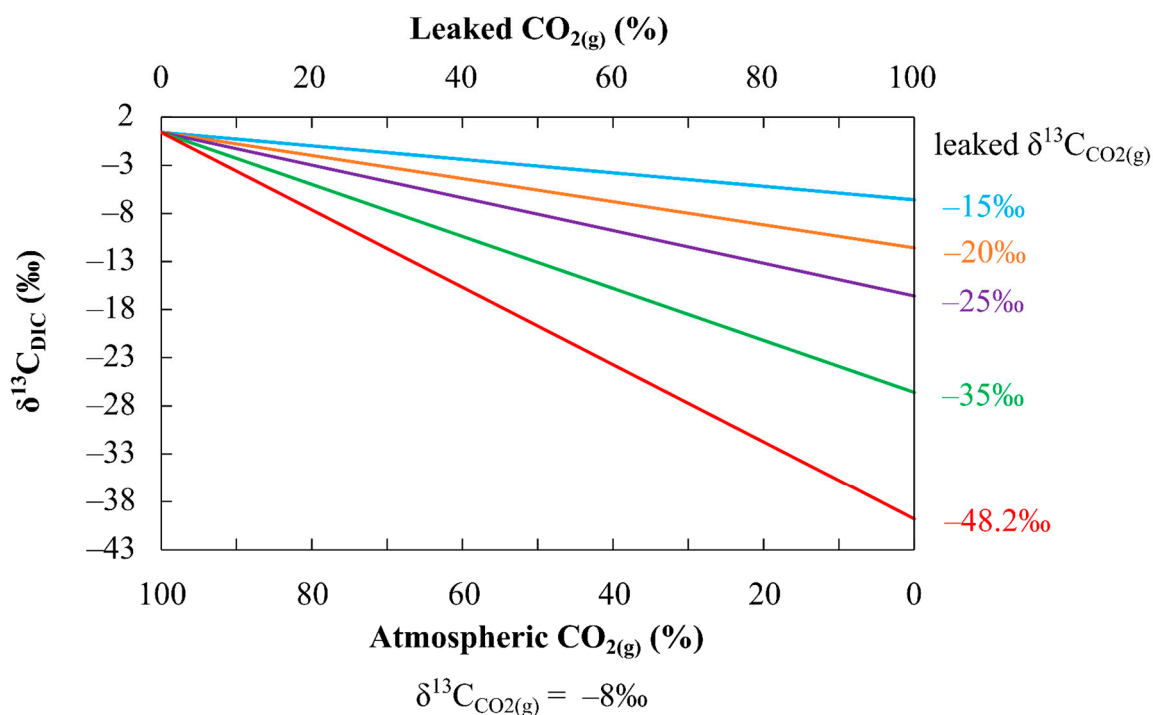


Figure 9. Predicted variation of $\delta^{13}\text{C}_{\text{DIC}}$ values according to the different $\delta^{13}\text{C}$ of leaking $\text{CO}_2(\text{g})$ from carbon capture and storage sites (CCS) and to the different proportions of DIC composed by leaking or atmospheric $\text{CO}_2(\text{g})$. The plots were produced applying the equation by Zhang et al. [76] assuming an atmospheric $\delta^{13}\text{C}_{\text{CO}_2(\text{g})}$ corresponding to -8.0‰ and using different leaking $\delta^{13}\text{C}_{\text{CO}_2(\text{g})}$ values: -15.0‰ (blue line), -20.0‰ (orange line), -25.0‰ (purple line) and -35.0‰ (green line). The $\delta^{13}\text{C}$ value of $\text{CO}_2(\text{g})$ used for the ASW experiments (-48.2‰) was also included (red line).

The variation of $\delta^{13}\text{C}_{\text{DIC}}$ calculated might slightly overestimate the final $\delta^{13}\text{C}_{\text{DIC}}$ in case the whole DIC derives from the leaked $\text{CO}_2(\text{g})$. Indeed, assuming that the DIC completely derives from the dissolution of $\text{CO}_2(\text{g})$ used for the experiments (-48.2‰), the calculated $\delta^{13}\text{C}_{\text{DIC}}$ result is -39.8‰ (Figure 9), which is higher than the measured $\delta^{13}\text{C}_{\text{DIC}}$ at the beginning of the three ASW experiments ($-44.2\text{‰} \pm 0.9\text{‰}$), but it still falls within the limits of the expected range. The equation by Zhang et al. [76], however, assumes that pH is constant and represents the results of the complete mixing of the water mass after leaking $\text{CO}_2(\text{g})$ dissolves and reaches equilibrium; thus, it does not reproduce the leakage conditions.

As highlighted by the release experiment by Blackford et al. [10], the porewater $\delta^{13}\text{C}_{\text{DIC}}$ values are modified earlier than the detection of significant changes in the bicarbonate concentration and more consistently than the water column $\delta^{13}\text{C}_{\text{DIC}}$ by $\text{CO}_2(\text{g})$ leakages. The direct monitoring of the changes in the $\delta^{13}\text{C}_{\text{DIC}}$ could therefore result not sufficient in detecting transient leaks because of carbonate buffering and of the rapid mixing in the surrounding environment of $\text{CO}_2(\text{g})$ leaking from a storage site. The primary producers' isotopic composition, instead, could represent a record of the changes induced by $\text{CO}_2(\text{g})$ leakage, because their isotopic composition directly depends on the $\delta^{13}\text{C}$ of the available DIC pool. Despite that phytoplankton could vertically migrate along the water column [52] and, thus, represents an important record of the modifications occurring in $\delta^{13}\text{C}_{\text{DIC}}$ after $\text{CO}_2(\text{g})$ leakages, these organisms are not able to contrast the strong currents that eventually can transport them horizontally far from the leakage site. Moreover, our experiments were conducted in a model case approach, where the whole carbonate system isotopic composition was modified and a single diatom species was tested, maintaining the pH levels within the natural range to allow phytoplankton optimal growth. Since storage sites will be predominantly hosted in coastal and shelf seas [11], and simulation results showed that the highest variations due to $\text{CO}_2(\text{g})$ leakages are predicted to affect the seabed [113], further experiments and investigations should be performed focusing on

tycopelagic and benthic primary producers (microalgae and/or seagrass) that are less prone to water currents. Moreover, benthic primary producers represent reliable biomonitoring because of the low spatial movement ability and would allow easier detection of transient and small leakages, since they live attached to the seafloor through which CO_{2(g)} is leaking.

For the future applications of this method, transient leakages characterised by different $\delta^{13}\text{C}$ of injected CO_{2(g)} should be explored, both by culture and release field experiments, and a multispecies approach should also be tested to consider the interspecific variability of carbon isotopic fractionation. As already highlighted in other studies (e.g., [5,10,21,22]), it is critical to extensively define the natural baseline at the storage site from both a geochemical and biological perspective. The seasonal changes that naturally characterise phytoplankton and DIC isotopic composition [32,33] and seabed community cycles [10] should be deeply understood to allow the correct identification of leakages and not misinterpret the observed deviations. Furthermore, for the coastal storage sites, the definition of the natural baseline would be even more challenging and important, since the anthropogenic and riverine inputs and the higher productivity of these areas represent additional factors that strongly affect the phytoplankton and DIC $\delta^{13}\text{C}$ [10,33,114]. Moreover, the isotopic baseline should be defined, including the recent monitoring data, to take into account the decrease induced on the $\delta^{13}\text{C}_{\text{DIC}}$ and $\delta^{13}\text{C}_{\text{POC}}$ by the Suess effect [99]. It has been demonstrated that the decrease in $\delta^{13}\text{C}_{\text{DIC}}$ because of the invasion of anthropogenic CO_{2(g)} from the atmosphere is already responsible for the decrease in $\delta^{13}\text{C}_{\text{POC}}$ by an extra 0.5–0.8‰ consistently for every cell size [99].

5. Conclusions

The experiments presented here reveal that the primary producer's isotopic composition quickly responds to changes in the seawater $\delta^{13}\text{C}_{\text{DIC}}$; thus, this approach represents a valuable contribution for ocean management in the evaluation of the impacts of CO_{2(g)} released from carbon storage sites. These results highlight the relevance of the application of a multidisciplinary approach that includes biological monitoring for the identification of CO_{2(g)} leakages, since the phytoplankton isotopic composition provides time-integrated information on the dissolved inorganic carbon pool, allowing the identification of sporadic emissions that could be hardly detected by seawater sampling. The definition of a detailed baseline is a primary requirement in this field to allow the identification of the seasonal changes that could interfere with the observed variations in the isotopic composition of both the seawater and primary producers.

Considering the importance and the urge to reduce climate change effects, research on CCS monitoring strategies represents a primary field of study in which the biological approach using inherent tracers is still underused and under-investigated. The results of the experiments described are encouraging for the future application of the analysis of the primary producer's carbon stable isotopic composition for monitoring CCS sites, and more effort deserves to be dedicated in this direction.

Supplementary Materials: The following are available online at <http://www.mdpi.com/2073-4441/12/12/3573/s1>: Figure S1: Time variation of inorganic nutrients (DIN and PO₄) during the three *T. rotula* culture experiments. Figure S2: Prokaryotes abundance and isotopic composition during the three *T. rotula* culture experiments. Data are available at PANGAEA®, doi: <https://doi.org/10.1594/PANGAEA.925185>.

Author Contributions: Conceptualisation, N.O., M.G. and C.D.V.; data curation, F.R., N.O. and M.G.; formal analysis, F.R., F.C., M.S.T., A.B., L.U. and B.K.; funding acquisition, P.D.N. and C.D.V.; investigation, F.R., M.G., F.C., M.S.T., A.B. and L.U.; methodology, N.O., M.G., F.C. and C.D.V.; project administration, C.D.V.; resources, N.O., M.G., F.C., M.S.T., A.B., P.D.N. and C.D.V.; supervision, N.O., M.G., P.D.N. and C.D.V.; validation, F.R., N.O., M.G. and C.D.V.; visualisation, F.R.; writing—original draft, F.R. and writing—review and editing, F.R., N.O., M.G., F.C., M.S.T., A.B., L.U., B.K. and C.D.V. All authors have read and agreed to the published version of the manuscript.

Funding: This work was conducted using the ECCSEL RI funded by the European Union's Horizon 2020 research and innovation program under grant agreement No. 675206. It also represents a part of the project J1-8156: "Stable isotopes in the study of the impact of increasing CO₂ levels on C and Hg cycling in coastal waters" financially supported by Slovenian Research Agency and EU project MASSTWIN—Spreading excellence and widening participation in support of mass spectrometry and related techniques in health, the environment and food analysis

(H2020, grant agreement No. 692241). The photobioreactors used for the experiments were acquired in the framework of the Acid.it project: “Science for mitigation and adaptation policies to ecological and socio-economic impacts of acidification on Italian seas” financially supported by the Italian Ministry of Education, University and Research. Part of the data presented in the paper have been included in the Ph.D. thesis of Federica Relitti.

Acknowledgments: We are grateful to Alfred Beran for providing the algal culture and for the support in the preparations of the experiments; Sergio Predonzani and Matteo Bazzaro for the valuable help in the experiments set-up and sampling; Martina Kralj for the nutrient analysis and Mauro Celussi for the prokaryotes analysis. The two anonymous reviewers are warmly acknowledged for their valuable and constructive comments that greatly helped to improve our manuscript.

Conflicts of Interest: The authors declare no conflict of interest.

Appendix A

For molecular phytoplankton species identification, 25 mL (~40,000 cells mL⁻¹) of the cell culture from the experiment was filtered on a 1.2- μ m cellulose filter and frozen on -80° C. Genomic DNA was isolated with the DNeasy Plant Mini Kit (Qiagen) according to the manufacturer’s instructions. The 5’ end region of the ribulose biphosphate carboxylase large subunit (*rbcl*) gene was amplified using primer pair *rbcl*66+ (5’-TTAAGGAGAAATAAATGTCTCAATCTG-3’) and *Dtrbcl*3R (5’-ACACCWGACATACGCATCCA-3’) [115,116]. The reaction tubes contained a 25- μ L mixture of 200 μ mol L⁻¹ of each deoxynucleotide, 0.3 μ mol L⁻¹ of each primer, 4-mM MgCl₂, 1X DreamTaq green buffer, 0.2 U of DreamTaq DNA polymerase (Thermo Fisher Scientific Inc., Waltham, MA, USA) and 0.5–1 ng of genomic DNA. PCR conditions were as follows: an initial denaturation step of 10 min at 95 $^{\circ}$ C, 35 cycles of 30s at 95 $^{\circ}$ C, 30s at 47 $^{\circ}$ C, 1 min at 72 $^{\circ}$ C and final extension step of 7 min at 72 $^{\circ}$ C. PCR-amplified products were purified with a MinElute PCR Purification Kit (Qiagen) according to the manufacturer’s instructions. Purified PCR products were sequenced at MacroGen Europe (Amsterdam, The Netherlands). The resulting sequences (from both ends) were aligned using Geneious 7.1.7. software [117]. BLAST [118] was used for the searches and comparisons of the GenBank database [119].

Using the *rbcl* gene as a DNA barcode, we confirmed the species identity as *Thalassiosira rotula*. A new *Thalassiosira rbcl* nucleotide sequence was deposited in GenBank under accession number: MG214782.

References

1. UNFCCC. *Report of the Conference of the Parties on Its Twenty-First Session, Held in Paris from 30 November to 13 December 2015. Decision 1/CP.21. Report no.: FCCC/CP/2015/10 Add. 1.* 2015. Available online: <https://unfccc.int/resource/docs/2015/cop21/eng/10a01.pdf> (accessed on 18 December 2020).
2. Haszeldine, R.S.; Flude, S.; Johnson, G.; Scott, V. Negative emissions technologies and carbon capture and storage to achieve the Paris Agreement commitments. *Philos. Trans. R. Soc. A Math. Phys. Eng. Sci.* **2018**, *376*, 20160447. [CrossRef]
3. Blackford, J.C.; Alendal, G.; Avlesen, H.; Brereton, A.; Cazenave, P.W.; Chen, B.; Dewar, M.; Holt, J.; Phelps, J. Impact and detectability of hypothetical CCS offshore seep scenarios as an aid to storage assurance and risk assessment. *Int. J. Greenh. Gas Control* **2020**, *95*, 102949. [CrossRef]
4. IPCC. IPCC special report on carbon dioxide capture and storage. In *Working Group III of the Intergovernmental Panel on Climate Change*; Metz, B., Davidson, O., de Coninck, H.C., Loos, M., Meyer, L.A., Eds.; Cambridge University Press: Cambridge, UK; New York, NY, USA, 2005.
5. Flude, S.; Johnson, G.; Gilfillan, S.M.V.; Haszeldine, R.S. Inherent tracers for carbon capture and storage in sedimentary formations: Composition and applications. *Environ. Sci. Technol.* **2016**, *50*, 7939–7955. [CrossRef]
6. IEAGHG. *CCS Industry Build-out Rates—Comparison with Industry Analogues*; Report No.: 2017-TR6; IEAGHG: Cheltenham, UK, 2017.
7. Global CCS Institute. *Global status of CCS*; Global CCS Institute: Melbourne, VIC, Australia, 2019.
8. IEAGHG. *Review of Offshore Monitoring for CCS Projects*; IEAGHG: Cheltenham, UK, 2015.

9. Roberts, J.J.; Stalker, L. What have we learnt about CO₂ leakage from CO₂ release field experiments, and what are the gaps for the future? *Earth-Sci. Rev.* **2020**, *209*, 102939. [[CrossRef](#)]
10. Blackford, J.C.; Stahl, H.; Bull, J.M.; Bergès, B.J.P.; Cevatoglu, M.; Lichtschlag, A.; Connelly, D.; James, R.H.; Kita, J.; Long, D.; et al. Detection and impacts of leakage from sub-seafloor deep geological carbon dioxide storage. *Nat. Clim. Chang.* **2014**, *4*, 1011–1016. [[CrossRef](#)]
11. Jones, D.G.; Beaubien, S.E.; Blackford, J.C.; Foekema, E.M.; Lions, J.; De Vittor, C.; West, J.M.; Widdicombe, S.; Hauton, C.; Queirós, A.M. Developments since 2005 in understanding potential environmental impacts of CO₂ leakage from geological storage. *Int. J. Greenh. Gas Control* **2015**, *40*, 350–377. [[CrossRef](#)]
12. Noble, R.R.P.; Stalker, L.; Wakelin, S.A.; Pejic, B.; Leybourne, M.I.; Hortle, A.L.; Michael, K. Biological monitoring for carbon capture and storage—a review and potential future developments. *Int. J. Greenh. Gas Control* **2012**, *10*, 520–535. [[CrossRef](#)]
13. Shi, D.; Xu, Y.; Hopkinson, B.M.; Morel, F.M.M. Effect of ocean acidification on iron availability to marine phytoplankton. *Science* **2010**, *327*, 676–679. [[CrossRef](#)]
14. Kim, H.; Kim, Y.H.; Kang, S.G.; Park, Y.G. Development of environmental impact monitoring protocol for offshore carbon capture and storage (CCS): A biological perspective. *Environ. Impact Assess. Rev.* **2016**, *57*, 139–150. [[CrossRef](#)]
15. Gao, K.; Beardall, J.; Häder, D.P.; Hall-Spencer, J.M.; Gao, G.; Hutchins, D.A. Effects of ocean acidification on marine photosynthetic organisms under the concurrent influences of warming, UV radiation, and deoxygenation. *Front. Mar. Sci.* **2019**, *6*, 1–18. [[CrossRef](#)]
16. Li, F.; Beardall, J.; Collins, S.; Gao, K. Decreased photosynthesis and growth with reduced respiration in the model diatom *Phaeodactylum tricornutum* grown under elevated CO₂ over 1800 generations. *Glob. Chang. Biol.* **2017**, *23*, 127–137. [[CrossRef](#)]
17. Gao, K.; Campbell, D.A. Photophysiological responses of marine diatoms to elevated CO₂ and decreased pH: A review. *Funct. Plant Biol.* **2014**, *41*, 449–459. [[CrossRef](#)]
18. Liu, N.; Beardall, J.; Gao, K. Elevated CO₂ and associated seawater chemistry do not benefit a model diatom grown with increased availability of light. *Aquat. Microb. Ecol.* **2017**, *79*, 137–147. [[CrossRef](#)]
19. Eberlein, T.; Wohlrab, S.; Rost, B.; John, U.; Bach, L.T.; Riebesell, U.; Van De Waal, D.B. Effects of ocean acidification on primary production in a coastal North Sea phytoplankton community. *PLoS ONE* **2017**, *12*, 1–15. [[CrossRef](#)]
20. Tait, K.; Stahl, H.; Taylor, P.; Widdicombe, S. Rapid response of the active microbial community to CO₂ exposure from a controlled sub-seabed CO₂ leak in Ardmucknish Bay (Oban, Scotland). *Int. J. Greenh. Gas Control* **2015**, *38*, 171–181. [[CrossRef](#)]
21. Cao, C.; Liu, H.; Hou, Z.; Mehmood, F.; Liao, J.; Feng, W. A review of CO₂ storage in view of safety and cost-effectiveness. *Energies* **2020**, *13*, 600. [[CrossRef](#)]
22. Blackford, J.C.; Bull, J.M.; Cevatoglu, M.; Connelly, D.; Hauton, C.; James, R.H.; Lichtschlag, A.; Stahl, H.; Widdicombe, S.; Wright, I.C. Marine baseline and monitoring strategies for carbon dioxide capture and storage (CCS). *Int. J. Greenh. Gas Control* **2015**, *38*, 221–229. [[CrossRef](#)]
23. Mancinelli, G.; Vizzini, S. Assessing anthropogenic pressures on coastal marine ecosystems using stable CNS isotopes: State of the art, knowledge gaps, and community-scale perspectives. *Estuar. Coast. Shelf Sci.* **2015**, *156*, 195–204. [[CrossRef](#)]
24. Coplen, T.B. Guidelines and recommended terms for expression of stable-isotope-ratio and gas-ratio measurement results. *Rapid Commun. Mass Spectrom.* **2011**, *25*, 2538–2560. [[CrossRef](#)]
25. Mayer, B.; Humez, P.; Becker, V.; Dalkhaa, C.; Rock, L.; Myrtilinen, A.; Barth, J.A.C. Assessing the usefulness of the isotopic composition of CO₂ for leakage monitoring at CO₂ storage sites: A review. *Int. J. Greenh. Gas Control* **2015**, *37*, 46–60. [[CrossRef](#)]
26. Shin, W.J.; Ryu, J.S.; Choi, H.B.; Yun, S.T.; Lee, K.S. Monitoring the movement of artificially injected CO₂ at a shallow experimental site in Korea using carbon isotopes. *J. Environ. Manag.* **2020**, *258*, 110030. [[CrossRef](#)]
27. Flude, S.; Györe, D.; Stuart, F.M.; Zurakowska, M.; Boyce, A.J.; Haszeldine, R.S.; Chalaturnyk, R.; Gilfillan, S.M.V. The inherent tracer fingerprint of captured CO₂. *Int. J. Greenh. Gas Control* **2017**, *65*, 40–54. [[CrossRef](#)]
28. Warwick, P.D.; Ruppert, L.F. Carbon and oxygen isotopic composition of coal and carbon dioxide derived from laboratory coal combustion: A preliminary study. *Int. J. Coal Geol.* **2016**, *166*, 128–135. [[CrossRef](#)]

29. Hellevang, H.; Aagaard, P. Constraints on natural global atmospheric CO₂ fluxes from 1860 to 2010 using a simplified explicit forward model. *Sci. Rep.* **2015**, *5*, 1–12. [[CrossRef](#)]
30. Keeling, C.D. The Suess effect: ¹³Carbon-¹⁴Carbon interrelations. *Environ. Int.* **1979**, *2*, 229–300. [[CrossRef](#)]
31. Zeebe, R.E.; Wolf-Gladrow, D.A. *CO₂ in Seawater: Equilibrium, Kinetics, Isotopes*; Oceanography Series 65; Elsevier Science B.V.: Amsterdam, The Netherlands, 2001.
32. Magozzi, S.; Yool, A.; Vander Zanden, H.B.; Wunder, M.B.; Trueman, C.N. Using ocean models to predict spatial and temporal variation in marine carbon isotopes. *Ecosphere* **2017**, *8*, e01763. [[CrossRef](#)]
33. McMahon, K.W.; Hamady, L.L.; Thorrold, S.R. A review of ecogeochemistry approaches to estimating movements of marine animals. *Limnol. Oceanogr.* **2013**, *58*, 697–714. [[CrossRef](#)]
34. Cheng, L.; Normandeau, C.; Bowden, R.; Doucett, R.; Gallagher, B.; Gillikin, D.P.; Kumamoto, Y.; McKay, J.L.; Middlestead, P.; Ninnemann, U.; et al. An international intercomparison of stable carbon isotope composition measurements of dissolved inorganic carbon in seawater. *Limnol. Oceanogr. Methods* **2019**, *17*, 200–209. [[CrossRef](#)]
35. Mook, W.G.; Bommerson, J.C.; Staverman, W.H. Carbon isotope fractionation between dissolved bicarbonate and gaseous carbon dioxide. *Earth Planet. Sci. Lett.* **1974**, *22*, 169–176. [[CrossRef](#)]
36. Raven, J.A. Physiology of inorganic C acquisition and implications for resource use efficiency by marine phytoplankton: Relation to increased CO₂ and temperature. *Plant. Cell Environ.* **1991**, *14*, 779–794. [[CrossRef](#)]
37. Tcherkez, G.G.B.; Farquhar, G.D.; Andrews, T.J. Despite slow catalysis and confused substrate specificity, all ribulose biphosphate carboxylases may be nearly perfectly optimized. *Proc. Natl. Acad. Sci. USA* **2006**, *103*, 7246–7251. [[CrossRef](#)]
38. Baird, M.E. Using a phytoplankton growth model to predict the fractionation of stable carbon isotopes. *J. Plankton Res.* **2001**, *23*, 841–848. [[CrossRef](#)]
39. Laws, E.A.; Popp, B.N.; Bidigare, R.R.; Kennicutt, M.C.; Macko, S.A. Dependence of phytoplankton carbon isotopic composition on growth rate and [CO₂]_{aq}: Theoretical considerations and experimental results. *Geochim. Cosmochim. Acta* **1995**, *59*, 1131–1138. [[CrossRef](#)]
40. Popp, B.N.; Laws, E.A.; Bidigare, R.R.; Dore, J.E.; Hanson, K.L.; Wakeham, S.G. Effect of phytoplankton cell geometry on carbon isotopic fractionation. *Geochim. Cosmochim. Acta* **1998**, *62*, 69–77. [[CrossRef](#)]
41. Bidigare, R.R.; Fluegge, A.; Freeman, K.H.; Hanson, K.L.; Hayes, J.M.; Hollander, D.; Jasper, J.P.; King, L.L.; Laws, E.A.; Milder, J.; et al. Consistent fractionation of ¹³C in nature and in the laboratory: Growth-rate effects in some haptophyte algae. *Glob. Biogeochem. Cycles* **1997**, *11*, 279–292.
42. Nimer, N.A.; Merrett, M.J. Calcification rate in *Emiliania huxleyi* Lohmann in response to light, nitrate and availability of inorganic carbon. *New Phytol.* **1993**, 673–677. [[CrossRef](#)]
43. Nimer, N.A.; Iglesias-Rodríguez, M.D.; Merrett, M.J. Bicarbonate utilization by marine phytoplankton species. *J. Phycol.* **1997**, *33*, 625–631. [[CrossRef](#)]
44. Burkhardt, S.; Riebesell, U.; Zondervan, I. Effects of growth rate, CO₂ concentration, and cell size on the stable carbon isotope fractionation in marine phytoplankton. *Geochim. Cosmochim. Acta* **1999**, *63*, 3729–3741. [[CrossRef](#)]
45. Yoshioka, T. Phytoplanktonic carbon isotope fractionation: Equations accounting for CO₂-concentrating mechanisms. *J. Plankton Res.* **1997**, *19*, 1455–1476. [[CrossRef](#)]
46. Sharkey, T.D.; Berry, J.A. Carbon isotope fractionation of algae as influenced by an inducible CO₂ concentrating mechanism. In *Inorganic Carbon Uptake by Aquatic Photosynthetic Organisms*; Lucas, W.J., Berry, J.A., Eds.; The American Society of Plant Physiologists: Rockville, MD, USA, 1985; pp. 389–401.
47. Falkowski, P.G. Species variability in the fractionation of ¹³C and ¹²C by marine phytoplankton. *J. Plankton Res.* **1991**, *13*, 21–28. [[CrossRef](#)]
48. Ha, J.H.; Jeon, S.W.; Hwang, H.T.; Lee, K.K. Changes in geochemical and carbon isotopic compositions during reactions of CO₂-saturated groundwater with aquifer materials. *Int. J. Greenh. Gas Control* **2020**, *95*, 102961. [[CrossRef](#)]
49. Mayer, B.; Shevalier, M.; Nightingale, M.; Kwon, J.-S.; Johnson, G.; Raistrick, M.; Hutcheon, I.; Perkins, E. Tracing the movement and the fate of injected CO₂ at the IEA GHG Weyburn-Midale CO₂ monitoring and storage project (Saskatchewan, Canada) using carbon isotope ratios. *Int. J. Greenh. Gas Control* **2013**, *16*, S177–S184. [[CrossRef](#)]
50. Jeandel, E.; Battani, A.; Sarda, P. Lessons learned from natural and industrial analogues for storage of carbon dioxide. *Int. J. Greenh. Gas Control* **2010**, *4*, 890–909. [[CrossRef](#)]

51. Shitashima, K.; Maeda, Y.; Sakamoto, A. Detection and monitoring of leaked CO₂ through sediment, water column and atmosphere in a sub-seabed CCS experiment. *Int. J. Greenh. Gas Control* **2015**, *38*, 135–142. [[CrossRef](#)]
52. Wirtz, K.; Smith, S.L. Vertical migration by bulk phytoplankton sustains biodiversity and nutrient input to the surface ocean. *Sci. Rep.* **2020**, *10*, 1142. [[CrossRef](#)]
53. Andersen, R.A. *Algal Culturing Techniques*; Elsevier: Amsterdam, The Netherlands, 2005.
54. Armbrust, E.V. The life of diatoms in the world's oceans. *Nature* **2009**, *459*, 185–192. [[CrossRef](#)]
55. Falkowski, P.G.; Barber, R.T.; Smetacek, V. Biogeochemical controls and feedbacks on ocean primary production. *Science* **1998**, *281*, 200–206. [[CrossRef](#)]
56. McClelland, H.L.O.; Bruggeman, J.; Hermoso, M.; Rickaby, R.E.M. The origin of carbon isotope vital effects in coccolith calcite. *Nat. Commun.* **2017**, *8*. [[CrossRef](#)]
57. Thronsen, J. Preservation and storage. In *Phytoplankton Manual. Monographs on Oceanographic Methodology 6*; Sournia, A., Ed.; UNESCO: Paris, France, 1978; pp. 69–74.
58. Gattuso, J.P.; Gao, K.; Lee, K.; Rost, B.; Schulz, K.G. Approaches and tools to manipulate the carbonate chemistry. In *Guide for Best Practices in Ocean Acidification Research and Data Reporting*; Riebesell, U., Fabry, V.J., Lina, H., Gattuso, J.P., Eds.; Office for Official Publications of the European Union: Luxemburg, 2010.
59. Dickson, A.G.; Sabine, C.; Christian, J.R. *Guide to Best Practices for Ocean CO₂ measurements. Standard operating Procedure (SOP) 3b, Determination of Total Alkalinity in Sea Water Using an Open-Cell Titration*; PICES Special Publication 3; IOCCP Report 8; North Pacific Marine Science Organization: Sidney, BC, Canada, 2007; 191p.
60. Ingrosso, G.; Giani, M.; Cibic, T.; Karuza, A.; Kralj, M.; Del Negro, P. Carbonate chemistry dynamics and biological processes along a river-sea gradient (Gulf of Trieste, northern Adriatic Sea). *J. Mar. Syst.* **2016**, *155*, 35–49. [[CrossRef](#)]
61. Hansen, H.; Koroleff, F. Determination of nutrients. In *Methods of Seawater Analysis*; Grasshoff, K., Kremling, K., Ehrhardt, M., Eds.; Wiley-VCH: Weinheim, Germany, 1999; pp. 159–228.
62. Pierrot, D.; Lewis, E.; Wallace, D. *MS Excel Program Developed for CO₂ System Calculations*; ORNL/CDIAC-105a; Carbon Dioxide Information Analysis Center, Oak Ridge National Laboratory, U.S. Department of Energy: Oak Ridge, TN, USA, 2006.
63. Mehrbach, C.; Culberson, C.; Hawley, J.; Pytkowics, R. Measurement of the apparent dissociation constants of carbonic acid in seawater at atmospheric pressure. *Limnol. Oceanogr.* **1973**, *18*, 897–907. [[CrossRef](#)]
64. Dickson, A.G.; Millero, F.J. A comparison of the equilibrium constants for the dissociation of carbonic acid in seawater media. *Deep Sea Res. Part A. Oceanogr. Res. Pap.* **1987**, *34*, 1733–1743. [[CrossRef](#)]
65. Dickson, A.G. Standard potential of the reaction: AgCl(s) + 12H₂(g) = Ag(s) + HCl(aq), and the standard acidity constant of the ion HSO₄[−] in synthetic sea water from 273.15 to 318.15 K. *J. Chem.* **1990**, *22*, 113–127. [[CrossRef](#)]
66. Uppström, L.R. The boron/chlorinity ratio of deep-sea water from the Pacific Ocean. *Deep Sea Res.* **1974**, *21*, 161–162. [[CrossRef](#)]
67. Marie, D.; Brussaard, C.P.D.; Thyrhaug, R.; Bratbak, G.; Vaultot, D. Enumeration of marine viruses in culture and natural samples by flow cytometry. *Appl. Environ. Microbiol.* **1999**, *65*, 45–52. [[CrossRef](#)]
68. Celussi, M.; Malfatti, F.; Annalisa, F.; Gazeau, F.; Giannakourou, A.; Pitta, P.; Tsiola, A.; Del Negro, P. Ocean acidification effect on prokaryotic metabolism tested in two diverse trophic regimes in the Mediterranean Sea. *Estuar. Coast. Shelf Sci.* **2017**, *186*, 125–138. [[CrossRef](#)]
69. Hasle, G.; Syvertson, E. Marine diatoms. In *Identifying Marine Phytoplankton*; Tomas, C., Ed.; Academic Press: Cambridge, MA, USA, 1997.
70. Rau, G.H.; Riebesell, U.; Wolf-Gladrow, D.A. A model of photosynthetic ¹³C fractionation by marine phytoplankton based on diffusive molecular CO₂ uptake. *Mar. Ecol. Prog. Ser.* **1996**, *133*, 275–285. [[CrossRef](#)]
71. Clark, I.D.; Fritz, P. (Eds.) *Environmental Isotopes in Hydrogeology*, 2nd ed.; CRC Press: Boca Raton, FL, USA; Taylor & Francis Group: Abingdon, UK, 1999; ISBN 1566702496.
72. Farquhar, G.D.; Ehleringer, J.R.; Hubick, K.T. Carbon isotope discrimination and photosynthesis. *Annu. Rev. Plant Physiol. Plant Mol. Biol.* **1989**, *40*, 503–537. [[CrossRef](#)]
73. Freeman, K.H.; Hayes, J.M. Fractionation of carbon isotopes by phytoplankton and estimates of ancient CO₂ levels. *Glob. Biogeochem. Cycles* **1992**, *6*, 185–198. [[CrossRef](#)]
74. Gat, J.R.; Gonfiantini, R. *Stable Isotope Hydrology. Deuterium and Oxygen-18 in the Water Cycle*; Technical Report 210; International Atomic Energy Agency: Vienna, Austria, 1981.

75. Laws, E.A.; Thompson, P.A.; Popp, B.N.; Bidigare, R.R. Sources of inorganic carbon for marine microalgal photosynthesis: A reassessment of $\delta^{13}\text{C}$ data from batch culture studies of *Thalassiosira pseudonana* and *Emiliania huxleyi*. *Limnol. Oceanogr.* **1998**, *43*, 136–142. [[CrossRef](#)]
76. Zhang, J.; Quay, P.D.; Wilbur, D.O. Carbon isotope fractionation during gas-water exchange and dissolution of CO_2 . *Geochim. Cosmochim. Acta* **1995**, *59*, 107–114. [[CrossRef](#)]
77. Clarke, K.; Gorley, R.; Somerfield, P.; Warwick, R. *Change in Marine Communities: An Approach to Statistical Analysis and Interpretation*, 3rd ed.; PRIMER-E: Plymouth, UK, 2014.
78. Ingrosso, G.; Bensi, M.; Cardin, V.; Giani, M. Anthropogenic CO_2 in a dense water formation area of the Mediterranean Sea. *Deep. Res. Part I Oceanogr. Res. Pap.* **2017**, *123*, 118–128. [[CrossRef](#)]
79. Tamše, S.; Ogrinc, N.; Walter, L.M.; Turk, D.; Faganeli, J. River sources of dissolved inorganic carbon in the Gulf of Trieste (N Adriatic): Stable carbon isotope evidence. *Estuaries Coasts* **2015**, *38*, 151–164. [[CrossRef](#)]
80. Bade, D.L.; Carpenter, S.R.; Cole, J.J.; Hanson, P.C.; Hesslein, R.H. Controls of $\delta^{13}\text{C}$ -DIC in lakes: Geochemistry, lake metabolism, and morphometry. *Limnol. Oceanogr.* **2004**, *49*, 1160–1172. [[CrossRef](#)]
81. Hinga, K.R. Effects of pH on coastal marine phytoplankton. *Mar. Ecol. Prog. Ser.* **2002**, *238*, 281–300. [[CrossRef](#)]
82. Clark, D.R.; Flynn, K.J. The relationship between the dissolved inorganic carbon concentration and growth rate in marine phytoplankton. *Proc. R. Soc. B Biol. Sci.* **2000**, *267*, 953–959. [[CrossRef](#)]
83. Clark, D.R.; Flynn, K.J.; Fabian, H. Variation in elemental stoichiometry of marine diatom *Thalassiosira weissflogii* (Bacillariophyceae) in response to combined nutrient stress and changes in carbonate chemistry. *J. Phycol.* **2014**, *50*, 640–651. [[CrossRef](#)]
84. Maugendre, L.; Gattuso, J.P.; Poulton, A.J.; Dellisanti, W.; Gaubert, M.; Guieu, C.; Gazeau, F. No detectable effect of ocean acidification on plankton metabolism in the NW oligotrophic Mediterranean Sea: Results from two mesocosm studies. *Estuar. Coast. Shelf Sci.* **2017**, *186*, 89–99. [[CrossRef](#)]
85. Esposito, M.; Achterberg, E.P.; Bach, L.T.; Connelly, D.P.; Riebesell, U.; Taucher, J. Application of stable carbon isotopes in a subtropical North Atlantic mesocosm study: A new approach to assess CO_2 effects in the marine carbon cycle. *Front. Mar. Sci.* **2019**, *6*, 616. [[CrossRef](#)]
86. Hurd, C.L.; Hepburn, C.D.; Currie, K.I.; Raven, J.A.; Hunter, K.A. Testing the effects of ocean acidification on algal metabolism: Consideration for experimental designs. *J. Phycol.* **2009**, *45*, 1236–1251. [[CrossRef](#)]
87. Li, F.; Fan, J.; Hu, L.; Beardall, J.; Xu, J.; Fields, D. Physiological and biochemical responses of *Thalassiosira weissflogii* (diatom) to seawater acidification and alkalization. *ICES J. Mar. Sci.* **2019**, *76*, 1850–1859. [[CrossRef](#)]
88. Giordano, M.; Beardall, J.; Raven, J.A. CO_2 concentrating mechanisms in algae: Mechanisms, environmental modulation, and evolution. *Annu. Rev. Plant Biol.* **2005**, *56*, 99–131. [[CrossRef](#)] [[PubMed](#)]
89. Shen, C.; Dupont, C.L.; Hopkinson, B.M. The diversity of CO_2 -concentrating mechanisms in marine diatoms as inferred from their genetic content. *J. Exp. Bot.* **2017**, *68*, 3937–3948. [[CrossRef](#)] [[PubMed](#)]
90. Colman, B.; Huertas, I.E.; Bhatti, S.; Dason, J.S. The diversity of inorganic carbon acquisition mechanisms in eukaryotic microalgae. *Funct. Plant Biol.* **2002**, *29*, 261–270. [[CrossRef](#)] [[PubMed](#)]
91. Burkhardt, S.; Amoroso, G.; Riebesell, U.; Sültemeyer, D. CO_2 and HCO_3^- uptake in marine diatoms acclimated to different CO_2 concentrations. *Limnol. Oceanogr.* **2001**, *46*, 1378–1391. [[CrossRef](#)]
92. Cozzi, S.; Falconi, C.; Comici, C.; Čermelj, B.; Kovac, N.; Turk, V.; Giani, M. Recent evolution of river discharges in the Gulf of Trieste and their potential response to climate changes and anthropogenic pressure. *Estuar. Coast. Shelf Sci.* **2012**, *115*, 14–24. [[CrossRef](#)]
93. Paul, A.J.; Bach, L.T.; Schulz, K.G.; Boxhammer, T.; Czerny, J.; Achterberg, E.P.; Hellemann, D.; Trense, Y.; Nausch, M.; Swat, M.; et al. Effect of elevated CO_2 on organic matter pools and fluxes in a summer Baltic Sea plankton community. *Biogeosciences* **2015**, *12*, 6181–6203. [[CrossRef](#)]
94. Li, F.; Wu, Y.; Hutchins, D.A.; Fu, F.; Gao, K. Physiological responses of coastal and oceanic diatoms to diurnal fluctuations in seawater carbonate chemistry under two CO_2 concentrations. *Biogeosciences* **2016**, *13*, 6247–6259. [[CrossRef](#)]
95. Tamše, S.; Mozetič, P.; Francé, J.; Ogrinc, N. Stable isotopes as a tool for nitrogen source identification and cycling in the Gulf of Trieste (Northern Adriatic). *Cont. Shelf Res.* **2014**, *91*, 145–157. [[CrossRef](#)]
96. Faganeli, J.; Ogrinc, N.; Kovac, N.; Kukovec, K.; Falnoga, I.; Mozetič, P.; Bajt, O. Carbon and nitrogen isotope composition of particulate organic matter in relation to mucilage formation in the northern Adriatic Sea. *Mar. Chem.* **2009**, *114*, 102–109. [[CrossRef](#)]

97. Giani, M.; Berto, D.; Rampazzo, F.; Savelli, F.; Alvisi, F.; Giordano, P.; Ravaioli, M.; Frascari, F. Origin of sedimentary organic matter in the north-western Adriatic Sea. *Estuar. Coast. Shelf Sci.* **2009**, *84*, 573–583. [[CrossRef](#)]
98. Poulain, C.; Lorrain, A.; Mas, R.; Gillikin, D.P.; Dehairs, F.; Robert, R.; Paulet, Y.M. Experimental shift of diet and DIC stable carbon isotopes: Influence on shell $\delta^{13}\text{C}$ values in the Manila clam *Ruditapes philippinarum*. *Chem. Geol.* **2010**, *272*, 75–82. [[CrossRef](#)]
99. Tuerena, R.E.; Ganeshram, R.S.; Humphreys, M.P.; Browning, T.J.; Bouman, H.; Piotrowski, A.P. Isotopic fractionation of carbon during uptake by phytoplankton across the South Atlantic subtropical convergence. *Biogeosciences* **2019**, *16*, 3621–3635. [[CrossRef](#)]
100. Henley, S.F.; Annett, A.L.; Ganeshram, R.S.; Carson, D.S.; Weston, K.; Crosta, X.; Tait, A.; Dougans, J.; Fallick, A.E.; Clarke, A. Factors influencing the stable carbon isotopic composition of suspended and sinking organic matter in the coastal Antarctic sea ice environment. *Biogeosciences* **2012**, *9*, 1137–1157. [[CrossRef](#)]
101. Coffin, R.B.; Fry, B.; Peterson, B.J.; Wright, R.T. Carbon isotopic compositions of estuarine bacteria. *Limnol. Oceanogr.* **1989**, *34*, 1305–1310. [[CrossRef](#)]
102. Hullar, M.; Fry, B.; Peterson, B.J.; Wright, R.T. Microbial utilization of estuarine dissolved organic carbon: A stable isotope tracer approach tested by mass balance. *Appl. Environ. Microbiol.* **1996**, *62*, 2489–2493. [[CrossRef](#)]
103. Lammers, J.M.; Reichart, G.J.; Middelburg, J.J. Seasonal variability in phytoplankton stable carbon isotope ratios and bacterial carbon sources in a shallow Dutch lake. *Limnol. Oceanogr.* **2017**, *62*, 2773–2787. [[CrossRef](#)]
104. De Kluijver, A.; Soetaert, K.; Schulz, K.G.; Riebesell, U.; Bellerby, R.G.J.; Middelburg, J.J. Phytoplankton-bacteria coupling under elevated CO_2 levels: A stable isotope labelling study. *Biogeosciences* **2010**, *7*, 3783–3797. [[CrossRef](#)]
105. Morales-Williams, A.M.; Wanamaker, A.D.; Downing, J.A. Cyanobacterial carbon concentrating mechanisms facilitate sustained CO_2 depletion in eutrophic lakes. *Biogeosciences* **2017**, *14*, 2865–2875. [[CrossRef](#)]
106. Boller, A.J.; Thomas, P.J.; Cavanaugh, C.M.; Scott, K.M. Isotopic discrimination and kinetic parameters of RubisCO from the marine bloom-forming diatom, *Skeletonema costatum*. *Geobiology* **2015**, *13*, 33–43. [[CrossRef](#)]
107. Young, J.N.; Bruggeman, J.; Rickaby, R.E.M.; Erez, J.; Conte, M. Evidence for changes in carbon isotopic fractionation by phytoplankton between 1960 and 2010. *Glob. Biogeochem. Cycles* **2013**, *27*, 505–515. [[CrossRef](#)]
108. Beardall, J.; Raven, J.A. The potential effects of global climate change on microalgal photosynthesis, growth and ecology. *Phycologia* **2004**, *43*, 26–40. [[CrossRef](#)]
109. Rayleigh, L. LIX. On the distillation of binary mixtures. *Lond. Edinb. Dublin Philos. Mag. J. Sci.* **1902**, *4*, 521–537. [[CrossRef](#)]
110. Ohkouchi, N.; Ogawa, N.O.; Chikaraishi, Y.; Tanaka, H.; Wada, E. Biochemical and physiological bases for the use of carbon and nitrogen isotopes in environmental and ecological studies. *Prog. Earth Planet. Sci.* **2015**, *2*, 1–17. [[CrossRef](#)]
111. Riebesell, U.; Wolf-Gladrow, D.A. Growth limits on phytoplankton. *Nature* **1995**, *373*, 28. [[CrossRef](#)]
112. Wang, S.; Yeager, K.M.; Lu, W. Carbon isotope fractionation in phytoplankton as a potential proxy for pH rather than for $[\text{CO}_2(\text{aq})]$: Observations from a carbonate lake. *Limnol. Oceanogr.* **2016**, *61*, 1259–1270. [[CrossRef](#)]
113. Pham, L.H.H.P.; Rusli, R.; Shariff, A.M.; Khan, F. Dispersion of carbon dioxide bubble release from shallow subsea carbon dioxide storage to seawater. *Cont. Shelf Res.* **2020**, *196*, 104075. [[CrossRef](#)]
114. Cotovicz, L.C.; Knoppers, B.A.; Deirmendjian, L.; Abril, G. Sources and sinks of dissolved inorganic carbon in an urban tropical coastal bay revealed by $\delta^{13}\text{C}$ -DIC signals. *Estuar. Coast. Shelf Sci.* **2019**, *220*, 185–195. [[CrossRef](#)]
115. Alverson, A.J. Molecular systematics and the diatom species. *Protist* **2008**, *159*, 339–353. [[CrossRef](#)]
116. MacGillivray, M.L.; Kaczmarek, I. Survey of the efficacy of a short fragment of the rbcL gene as a supplemental DNA barcode for diatoms. *J. Eukaryot. Microbiol.* **2011**, *58*, 529–536. [[CrossRef](#)]
117. Kearse, M.; Moir, R.; Wilson, A.; Stones-Havas, S.; Cheung, M.; Sturrock, S.; Buxton, S.; Cooper, A.; Markowitz, S.; Duran, C.; et al. Geneious basic: An integrated and extendable desktop software platform for the organization and analysis of sequence data. *Bioinformatics* **2012**, *28*, 1647–1649. [[CrossRef](#)]
118. Altschul, S. Gapped BLAST and PSI-BLAST: A new generation of protein database search programs. *Nucleic Acids Res.* **1997**, *25*, 3389–3402. [[CrossRef](#)] [[PubMed](#)]

119. Clark, K.; Karsch-Mizrachi, I.; Lipman, D.J.; Ostell, J.; Sayers, E.W. GenBank. *Nucleic Acids Res.* **2016**, *44*, D67–D72. [[CrossRef](#)] [[PubMed](#)]

Publisher’s Note: MDPI stays neutral with regard to jurisdictional claims in published maps and institutional affiliations.



© 2020 by the authors. Licensee MDPI, Basel, Switzerland. This article is an open access article distributed under the terms and conditions of the Creative Commons Attribution (CC BY) license (<http://creativecommons.org/licenses/by/4.0/>).